Interreg Alpine Space

Co-funded by the European Union

Alps4GreenC

Alps4GreenC
Deliverable 1.3.1
Alps4GreenC Testing and pilot production report

Results of experimental tests will be reported in this deliverable (feedstock analyses, laboratory tests, pilot tests, biochar analyses).

Authors:

Konstantin Moser (BEST)
Irene Sedlmayer (BEST)
Jure Voglar (NIC)
Borooah Rohit (unibz)

Date: February 29th 2024

Alps4GreenC partners:

NATIONAL INSTITUTE OF CHEMISTRY

ŠTAJERSKA GOSPODARSKA ZBORNICA

BEST Bioenergy and Sustainable Technologies

unibz Freie Universität Bozen Libera Università di Bolzano Università Liedia de Bulsan

BioBASE

AIEL ASSOCIAZIONE ITALIANA ENERGIE AGROFORESTALI

Contents

1 Introduction ... 3
2 Characterization of Residues ... 4
2.1 Results of Residue Characterization ... 5
3 Biochar Production ... 11
3.1 Pyrolysis ... 11
3.1.1 Sample Pretreatment ... 11
3.1.2 Lab-scale Pyrolysis ... 12
3.1.3 Pilot-scale Pyrolysis ... 17
3.2 Gasification ... 19
3.2.1 Sample Pretreatment ... 19
3.2.2 Lab-scale Gasification ... 20
3.2.3 Pilot-scale Gasification ... 26
4 Biochar Characterization ... 30
4.1 Results and Discussion ... 30
4.1.1 Basic Characterization ... 30
4.1.2 Elemental Composition ... 32
4.1.3 Other Biochar Properties ... 35
4.1.4 PAH Measurements ... 37
4.1.5 PCB & PCDD/PCDF Measurements ... 38
4.1.6 X-ray Powder Diffraction (XRD) ... 40
4.1.7 Thermogravimetry (TG) ... 43
4.1.8 pH Measurements ... 45
4.1.9 Scanning Electron Microscopy (SEM) ... 46
4.1.10 ATR-FTIR spectroscopy ... 49
5 Summary and Conclusion ... 52
5.1 Application in Steel and Agriculture ... 52
5.2 Outlook ... 53
6 Figures and Tables ... 54
7 References ... 58

1 Introduction

The Alps4GreenC project aims at implementing transnational value-chains in the Alpine territories to facilitate the development and implementation of bio-economy focusing mainly on the sustainable production and utilization of green carbon, especially biochar.

Therefore, project tasks not only foreseen practical tests for biochar production, but also mapping activities, context and gap analyses and policy recommendations.
In order to collect the biomass residues to be converted into biochar, facilitate the mapping and raise awareness among citizens, companies, and other stakeholders on the benefits of green carbon utilization, a crowdsourcing campaign was launched in the three countries involved in the project: Austria, Italy and Slovenia.

In the course of the activity 1.3 Practical testing and pilot production of green carbon the Deliverable 1.3.1 Alps4GreenC Testing and pilot production report is created.
This report presents the methodology used for residue analyses, laboratory tests, pilot tests and biochar analyses. Based on analyses results, 10 residues are selected for laboratory tests (5 for gasification tests at unibz, 5 for pyrolysis tests at BEST). Afterwards, tests at pilot scale are conducted (pyrolysis of 1 residue at BEST, gasification of 1 residue at unibz). The produced biochars in lab and pilot tests are sent to NIC for analyses and evaluation of its suitability for sustainable use in agriculture and steel industry. Further biochar analyses are performed from the external laboratory Water&Life Lab (Italy) and the project partner unibz.
BEST coordinated the report and the partners NIC and unibz supported the report with discussions and exchanges to share know-how on tests and processes.

2 Characterization of Residues

Out of the contenders of the crowdsourcing campaign, ten residues in total were set for thermochemical conversion, as described in more detail in deliverable 1.1.1. Table 1 gives an overview of the investigated residues and their origin.

Table 1 Selected residues and their source

Code	Residues	Conversion technology	Scale of Reactor	Participant	Country
1	Coffee husks	Pyrolysis	Laboratory	Atlantic Droga Kolinska d.o.o.	Slovenia
2	River woody debris	Gasification	Laboratory	Dravske elektrarne Maribor d.o.o.	Slovenia
3	Walnut shells	Pyrolysis	Laboratory + Pilot	NUSSLAND GmbH	Austria
4	Bran (starch)	Pyrolysis	Laboratory	Agrana Research & Innovation Center GmbH	Austria
5	Compost screenings	Pyrolysis	Laboratory	Brantner Österreich GmbH	Austria
6	Spelt husks	Gasification	Laboratory	Karl Brader	Austria
7	Wood affected by bark beetles	Gasification	Laboratory + Pilot	Dapoz Roland	Italy
8	Chestnut wood without tannins	Gasification	Laboratory	Ledoga srl	Italy
9	Vine prunings	Gasification	Laboratory	Az. Agr. Corte Arano di Giovannini Mattia	Italy
10	Wood chips from broadleaf forestry sites	Pyrolysis	Laboratory	BIOMASS GREEN ENERGY SRL	Italy

Before the thermochemical conversion tests started, all the selected residues were analyzed thoroughly, with AIEL being responsible for this task. The laboratory that performed the analyses was the *Water & Life Lab, Via Enrico Mattei n°37, 24060 - Entratico (BG) – ITALY.* The analyzes can be summarized in three different groups, with the results being shown in Table 2 to Table 6:

- General residue characterization
- Heavy metal and inorganic nutrient contents
- Particle size analyses

General residue characterization covers moisture content, ash and volatile matter content, elemental analyses for C/H/N/S/Cl, heating value, bulk density and ash melting behavior (this

was only done for gasification, as the temperature used for pyrolysis should not melt the ashes). Particle size analyses covers the particle size distribution of the residues. Both general residue characterization and particle size distribution were necessary to determine whether the residues were suitable for the process, or if any pretreatments would have been necessary. Moreover, heavy metal and nutrient analyses were performed to determine if any elements would be influenced by the thermochemical conversion, either through emission or contamination.

These residues were selected to reflect the participation in the crowdsourcing campaign described in deliverable 1.1.1, which resulted in 2 residues from Slovenia, 4 residues from Austria and 4 residues from Italy. The following sections describe the residues selected and the motivation behind their selection.

2.1 Results of Residue Characterization

In general, the results from the residue analyses did not show anything unexpected or unusual. The results of general residue characterization are shown in Table 3 and Table 4. Looking at the main elemental constituents (carbon, hydrogen, oxygen and nitrogen), it can be seen that biomass residues differ in their elemental composition. While hydrogen hardly differed among the residues, with most of them being at around 6 w/w% $_{d.b.}$ (w/w% $_{d.b.}$ is for weight by weight in percentage on dry basis), carbon, oxygen and nitrogen did show considerable differences. For carbon the maximum value was found in the walnut shells with 49.0 w/w% $_{d.b.}$ and the minimum value was found in the compost screening surplus with 42.0 w/w% $_{d.b}$. The maximum oxygen was found in the tannin removed chestnut wood with 44.7 w/w% $_{d.b.}$ and the minimum was found in the compost screening surplus with 33.2 w/w% $_{d.b.}$. For nitrogen, the maximum amount was found in the coffee husks with 2.9 w/w% $_{d.b.}$ and the minimum was found in the bark beetle affected wood with 0.1 w/w% $_{d.b.}$ Chlorine was below 0.1 w/w% $_{d.b.}$ for all samples except the compost screening surplus that contained 0.58 w/w% $_{d.b.}$ chlorine. Sulphur was below 0.1 w/w% $_{d.b.}$ for all samples, except the walnut shells, the wheat bran and the compost screening surplus, each containing 0.28, 0.18 and 0.24 w/w% $_{d.b.}$ respectively. Ash, another main constituent of biomass, was also present in varying amounts. The maximum amount was found in the compost screening surplus with 16.94 w/w% $_{d.b}$, which is rather high for biomass and the minimum ash content was found in the tannin removed chestnut wood with 0.69 w/w% $_{d.b.}$. The high ash content in the compost screening surplus can be explained by the presence of inorganic parts like metals, sand and small stones., as is usual for a residue of this kind (Sieb-OPTI, *2020)*. The calorific values are typical for biomass, with values around ~14.4-18 MJ/kg $_{d.b.}$. Bulk density and moisture content also showed considerable variability.

As an additional step of quality insurance, the general fuel data was compared with available data from the Phyllis2 database. The database contained general fuel data for coffee husks, walnut shells, bran (starch), compost screening and vine prunings. Strong similarity was found, as can be seen in Table 2, further assuring the quality of analyses.

Table 2: Values gathered from residue analyses compared to data from the Phyllis2 database. All values are based on dry basis (d.b.) and given in % w/w, except for the gross calorific value, which is given in MJ/kg.

Parameter	**Alps4GreenC**	**Phyllis2**
	Coffee husks	
	Code 1	**#2307**
Ash content	7.32	11.61
Carbon	46.7	46.5
Hydrogen	6.1	6.3
Oxygen	36.6	35.0
Nitrogen	2.9	0.7
Gross calorific value	18.72	18.93
	Walnut Shells	
	Code 3	***#1435***
Ash content	1.23	0.56
Carbon	49.0	50.0
Hydrogen	5.9	5.7
Oxygen	43.4	43.4
Nitrogen	0.4	0.2
Sulphur	0.03	0.01
	Wheat Bran	
	Code 4	**#2389**
Ash content	7.08	7.00
Nitrogen	2.5	2.94
	Compost screening	
	Code 5	**#908**
Ash	16.94	20.14
Carbon	42.0	40.2
Hydrogen	5.2	4.1
Oxygen	33.2	34.6
Nitrogen	1.6	0.7
Sulphur	0.24	0.12
Gross calorific value	17.03	17.00
	Vine prunings	
	Code 9	**#3351**
Carbon	46.4	48.2
Hydrogen	6.0	5.6
Oxygen	43.1	42.8
Nitrogen	0.8	0.8
Gross calorific value	18.65	18.81

Regarding the heavy metal elements, it can be said that all the samples contained very little arsenic, thallium, mercury and cadmium, with most or in the case of thallium all the analyzed residues having concentrations below the limit of quantification of the method used. Lead,

nickel and chromium were present in detectable amounts with concentrations of <10 mg/kg $_{d.b.}$ for all samples. Manganese, copper and zinc showed the highest levels with some samples being <10 mg/kg $_{d.b.}$, most of the samples being between 10-100 mg/kg $_{d.b.}$ and in the case of manganese some samples even exceeding 100 mg/kg $_{d.b.}$ The nutrient elements P and K showed great variation between the analyzed residues. For phosphorous the maximum value found was 13259.0 mg/kg$_{d.b.}$ in the wheat bran and the minimum value was 28.5 mg/kg $_{d.b.}$ in the tannin removed chestnut wood. For potassium, the maximum value was 16747.2 mg/kg $_{d.b.}$ in the walnut shells and the minimum value was 108.7 mg/kg $_{d.b.}$ in the tannin removed chestnut wood. For all the data on heavy metal and nutrient contents see Table 5. The results of the particle size distribution can be seen in Table 6. It is clearly visible that the wheat bran has the smallest average particle size, with basically 100 % of it belonging to the <3.15 mm fraction. The vine prunings, on the other hand, showed the largest average particle size, with 51.5 % belonging to the >100 mm fraction.

Table 3: General properties of the analyzed residues

	Moisture	Ash at 550°	Bulk density	Carbon	Chlorine	Hydrogen	Oxygen	Nitrogen	Sulphur
Sample	**w-% d.b.**	**w-% d.b.**	**kg/m³**	**w-% d.b.**	**w-% d.b.**	**w-% d.b.**	**w-% d.b.**	**w-% d.b.**	**w-% d.b.**
1	25.04	7.32	342	46.7	0.06	6.1	36.6	2.9	0.28
2	26.27	1.70	217	47.6	< 0.01	6.0	44.4	0.3	0.04
3	11.78	1.23	286	49.0	0.04	5.9	43.4	0.4	0.03
4	10.70	7.08	386	44.2	0.06	6.4	39.6	2.5	0.18
5	7.07	16.94	231	42.0	0.58	5.2	33.2	1.6	0.24
6	10.01	7.05	153	43.4	0.008	5.8	43.2	0.4	0.07
7	3.89	0.96	185	48.4	0.01	6.1	44.4	0.1	<0.01
8	39.56	0.69	275	48.3	0.01	6.0	44.7	0.3	0.02
9	13.10	3.61	107	46.4	0.02	6.0	43.1	0.8	0.07
10	29.89	3.61	246	46.0	0.01	6.0	43.9	0.5	0.05
Methods used	ISO 14780: 2019 + ISO 18134-1: 2015	ISO 14780:2019 + ISO 18122: 2016	ISO 14780: 2019 + ISO 17828:2016	ISO1 6948: 2015	ISO 16994: 2017 Met A + ISO 10304-1: 2009	ISO 16948: 2015	calculated by difference	ISO 16948: 2015	ISO 16994: 2017 Met A + ISO 10304-1: 2009

Table 4: Calorific values for the different residues

	Gross calorific value	**Net calorific value**	**Gross calorific value**	**Net calorific value**
Sample	MJ/kg	MJ/kg	MJ/kg $_{d.b.}$	MJ/kg $_{d.b.}$
1	14.04	12.96	18.73	18.10
2	14.04	12.96	19.04	18.45
3	17.64	16.56	20.00	19.10
4	16.20	15.12	18.14	17.22
5	15.84	16.20	17.05	17.62
6	15.48	14.40	17.20	16.27
7	19.44	18.36	20.23	19.20
8	11.16	10.08	18.46	18.28
9	16.20	15.12	18.64	17.77
10	12.60	11.88	17.97	17.99
Methods used	ISO 18125: 2018	ISO 18125: 2018	calculated	calculated

*Table 5: Nutrient and heavy metal contents of the analyzed residues. All values in mg/kg $_{d.b.}$ * The starred Tests are not ACCREDIA qualified. The used methods: ISO 14780: 2019; ISO 16968:2015 and ISO 6170 :2016*

Sample	As	Cd	Cr	*Mn	Hg	Ni	Pb	Cu	*Tl	Zn	*P	*K
1	< 0.4	< 0.2	1.8	44.0	< 0.04	1.0	0.3	63.6	< 2.0	15.2	918.0	16747.2
2	< 0.4	0.2	6.4	74.9	< 0.04	3.2	1.9	3.1	< 2.0	21.0	171.3	615.6
3	< 0.4	< 0.2	1.8	7.0	< 0.04	1.2	< 0.2	3.4	< 2.0	5.0	305.8	2696.3
4	< 0.4	< 0.2	0.4	101.5	< 0.04	0.9	< 0.2	11.5	< 2.0	97.9	13259.0	12392.7
5	1.6	0.2	15.3	195.1	< 0.04	6.2	4.5	18.2	< 2.0	58.7	2169.5	13001.5
6	< 0.4	< 0.2	2.1	11.9	< 0.04	1.0	< 0.2	1.5	< 2.0	9.1	1892.2	3342.5
7	< 0.4	0.	3.6	50.0	< 0.04	2.2	3.0	8.7	< 2.0	27.0	38.6	674.3
8	< 0.4	< 0.2	5.7	35.1	< 0.04	2.8	0.8	2.0	< 2.0	7.4	28.5	108.7
9	< 0.4	< 0.2	3.8	34.5	< 0.04	2.4	0.5	11.7	< 2.0	37.3	1105.0	5685.1
10	< 0.4	0.3	2.8	15.6	< 0.04	1.4	0.5	5.8	< 2.0	29.4	540.1	2638.9

Table 6: Particle size distributions for the different samples. All values given in %. Methods used: ISO 14780: 2019; ISO 16968:2015 and ISO 6170: 2016

Sample	< 3.15 mm	3.15 - 16 mm	16 - 31.5 mm	31.5 - 45 mm	45 - 63 mm	63 - 100 mm	> 100 mm	Sum in %
1	12.9	85.9	0.0	0.0	0.0	0.0	0.0	98.8
2	2.9	24.8	38.7	18.5	5.3	0.0	8.7	98.9
3	1.6	17.0	80.1	0.9	0.0	0.0	0.0	99.7
4	99.9	0.0	0.0	0.0	0.0	0.0	0.0	99.9
5	33.1	57.8	6.4	1.9	0.0	0.0	0.0	99.2
6	87.4	12.6	0.0	0.0	0.0	0.0	0.0	100.0
7	3.3	31.5	51.7	9.8	1.7	0.0	1.9	99.9
8	8.3	74.5	15.6	0.5	0.0	0.0	0.0	98.9
9	1.3	11.4	7.5	4.9	1.3	22.1	51.5	99.9
10	3.7	27.2	50.4	9.9	2.0	0.0	5.1	98.1

3 Biochar Production

One of the main goals of this project was the production of biochar from different residues. Two thermochemical technologies were set to do this task: **Pyrolysis and Gasification**. Five of the selected residues were converted with each technology at lab scale, with one of those residues additionally being converted by a pilot scale plant (also see Table 1). The responsibility for the conversion tests was split between BEST and unibz, with BEST being responsible for pyrolysis testing and unibz being responsible for gasification testing.

3.1 Pyrolysis

3.1.1 Sample Pretreatment

After evaluating the quality of the results, it was also determined whether the residues were ready for conversion or if some additional pretreatment was necessary. For pyrolysis, no fundamental problem was found. However, the coffee husks and the wood chips from broadleaf forestry (samples 1 and 10) needed some treatment before the tests could start. Both residues were delivered in particle sizes too large for the lab-scale pyrolysis reactor and contained a problematic amount of moisture. For the wood chips, this is reflected in Table 6 with a considerable portion of the residue belonging to the fractions of 16 mm and above and a moisture content of ~30 w/w%. To overcome these issues, the wood chips were air-dried first (moisture of ~9 w/w%) and then sieved through a 16x16 mm mesh, located at BEST (Figure 1). For the coffee husks, the pretreatment was not that easy. As seen in Figure 2, the coffee husks were originally delivered as large briquettes, representing their final form after processing. These briquettes varied in physical rigidity, with some being rather brittle and others being very sturdy. This not only prevented them from being pyrolyzed, but also made it impossible to get reproduceable results in the particle size analysis. In addition to that, similar to the wood chips, they contained a lot of moisture (~25 w/w%) which caused molding in the batch stored at BEST. To address this, the lab responsible for analyses crushed the briquettes into smaller chunks with a powdery fraction, so the particle size analyses would yield reproduceable results. BEST requested a new batch from the provider, that was taken pre-briquetting, which also resulted in lower moisture content (see Table 7). The new batch of coffee husks (to be seen in Figure 2) was a lot finer and should more or less resemble the particle size distribution that was determined for the crushed briquettes in the lab.

Figure 1: The 16x16 mm sieve apparatus made by FleXiever located at BEST, used to sieve sample 10

Figure 2: Top: The coffee husks in their final form after processing; Bottom: The second batch of coffee husks at BEST, set for pyrolysis

3.1.2 Lab-scale Pyrolysis

The experimental setup

The lab-scale pyrolysis was performed on a small, custom-made plant, located at BEST in Wieselburg, Lower Austria. The system is a continuous rotary kiln, with the ability to adjust inclination and speed of rotation of the drum. It is electrically heated, with three separate heating elements being responsible for providing and sustaining the temperature in the reactor. The drum has a total length of 2.9 m and a heated length of 1.1 m, with a diameter of 0.27 m. It is a screw-fed system, with the residue storage being marked in Figure 3. The plant has a nominal capacity of 2.5 kg/h woodchips. The inclination of the drum can be varied between 0 and 10° and the speed of rotation can be varied between 1 and 11 revolutions per minute. The maximum temperature of the heating elements can sustain up to about 1000-1100 °C and a variable nitrogen flow (0-200 L/min) is provided through four different inlets, to ensure an oxygen-free reactor atmosphere.

Figure 3: The used rotary kiln system, with the residue storage marked in red.

Conducting the experiments

All experiments on the lab-scale equipment were conducted in July and August 2023. The project was intended to produce one biochar sample per residue, totaling five biochar samples from the lab-scale equipment. Before the test, each residue was tested for moisture content by heating to 103 °C until mass constancy was reached. Table 7 compares the moisture contents directly before the experiments and from residue analysis. It can be seen that all samples except 1 and 10 showed no considerable difference in moisture. The differences for samples 1 and 10 are explained in section 3.1.1.

Table 7: Moisture content of the residues selected for pyrolysis, measured before the experiment and during residue analyses

Code	Residue	Moisture before testing in w/w %	Moisture determined by residue analysis in w/w %
1	coffee husks	18.9	25.04
3	walnut shells	10.6	11.78
4	bran	10.9	10.70
5	compost screening	6.7	7.07
10	wood chips from broadleaf forestry sites	9.0	29.89

Before each test, the reactor was flushed with several hundred liters of nitrogen. Afterwards, the feeding screw was turned on and the experiment started. Table 8 shows the process parameters set for each experiment.

Table 8: Process parameters set for each sample during lab-scale pyrolysis

Code	Residue	Average nitrogen flow in L/min	Average Temperature in °C	Inclination in °	Speed of rotation in rpm
1	coffee husks	10.18 ± 9.40	507.23 ± 9.40	2	3
3	walnut shells	8.45 ± 4,78	506.44 ± 9.45	1	2
4	bran	22.09 ± 9.89	504.09 ± 10.07	1	2
5	compost screening	6.64 ± 2.27	505.34 ± 11.84	3	6
10	wood chips from broadleaf forestry sites	13.91 ± 6.19	505.12 ± 7.94	3	6

Nitrogen flow was adapted according to the pressure behavior in the reactor. The temperature in the reactor was aimed at 500 °C. However, due to intrinsic fluctuations of the heating elements and the process of pyrolysis being a dynamic one, deviations were inevitable. As the maximum temperature has a great impact on biochar properties, temperature fluctuations should be as little as possible. Thus, for all the experiments, a maximum temperature fluctuation of 500±20°C was achieved.

Complications during the process

The goal in the project was to produce one sample of biochar for each selected residue at lab-scale. For pyrolysis, this goal was reached, and the five required biochar samples were produced. However, the process did not always run smoothly, and some issues could be observed. The first issue observed was reserved to the wheat bran. Due to the pyrolytic behavior of the bran, it could not traverse the hot reactor zone. As seen in Figure 4, the bran got stuck at the beginning of the hot reactor zone, where the pyrolysis starts. It is not entirely clear what caused this accumulation, but it was assumed that a combination of residue type and form is the primary cause. Only a small amount of biochar was exiting the reactor during the process, so after some time it was stopped. After the experiment, the reactor was opened at the biochar exit and the biochar accumulation was recovered mechanically.

Figure 4: A picture of the reactor inside, taken from the exit of the drum. It represents the beginning of the heated reactor zone, where clearly visible the bran biochar accumulated

The second issue was observed for all experiments and was related to the reactor setup. Figure 5 shows a detailed drawing of the used reactor, and where the reaction happens. Based on how the plant was operated, it was planned to remove the produced syngas through a hollow pipe inserted into the hot zone of the reactor (marked in orange). A constant flow of nitrogen should ensure that the syngas leaves the reactor in the hot zone and does not spread to the cool zones. However, it turned out that the concept did not work as intended. For one, the gas outlet in the reactor got plugged with biochar particles (Figure 6A) and secondly, the nitrogen flow was not able to contain the syngas in the hot reactor zone. This led to syngas condensing in the cool reactor zones, which resulted in black tar deposits in these areas, as can be seen in Figure 6B. Two intuitive solutions come to mind: 1. Improve the gas outlet, so it is less prone to being plugged, 2. Increase the temperature at the cool zones of the reactor, so no condensation happens. While both options will be considered in the future, it was unfortunately not possible to implement them during the project, as both require considerable engineering and validation efforts.

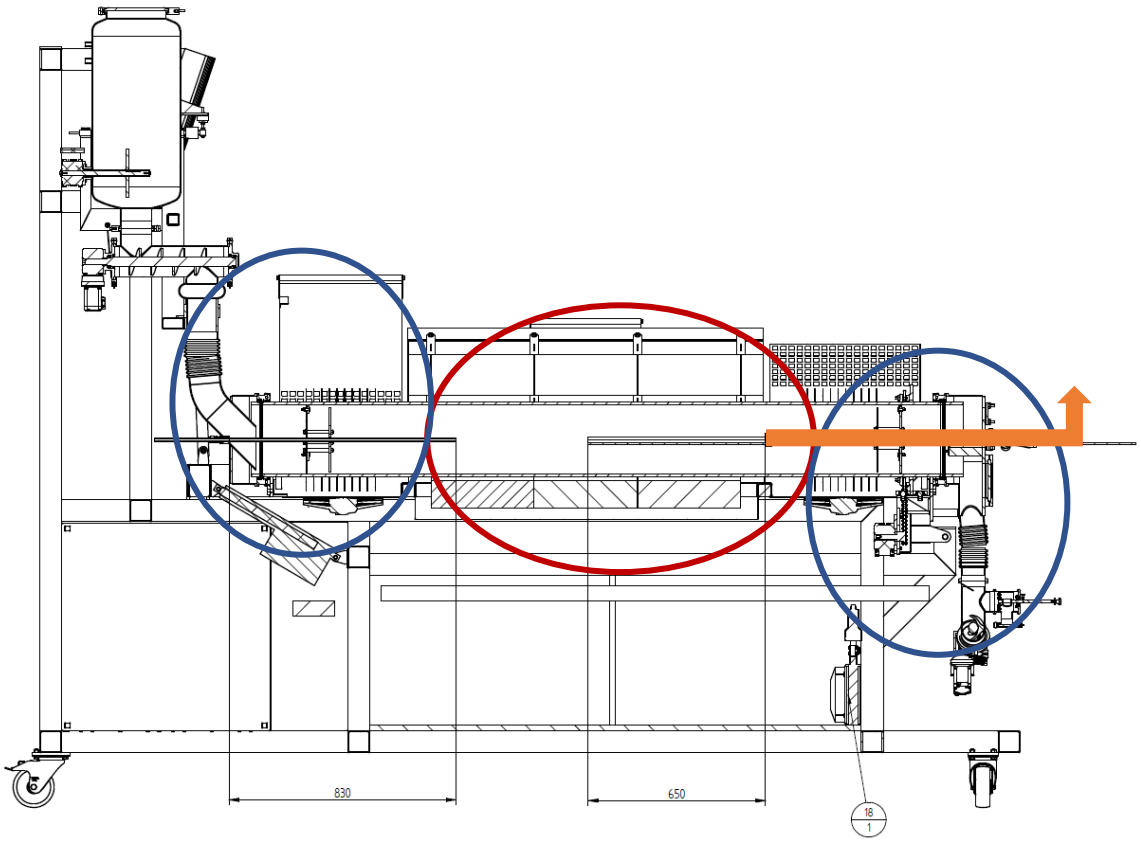

Figure 5: A detailed drawing of the lab-scale pyrolysis reactor. Marked in red is the hot zone of the reactor, marked in blue are the cool zones and marked in orange is the gas exit.

Figure 6: A) Picture of the gas outlet located in the hot reactor core. It can be clearly seen that the exit for the syngas is blocked by biochar particles. B) Exemplary picture of the tar deposition issue, located at the feeding screw

A third, but less critical issue was the occurrence of residue size related blockades of the feeding system. These mainly occurred for residues 5 and 10 and while they could always be resolved, for future experiments it is recommended to use smaller particle sizes to ensure a smooth operation. The final results of the lab scale pyrolysis are shown in Table 9.

*Table 9: Results of the lab scale pyrolysis experiments. *including maintenance breaks*

Code	Residue	Moisture biochar in w/w%	Yield in w/w % d.b.	Total time of experiment* in hh:mm:ss
1	coffee husks	12,3	27,8	03:37:27
3	walnut shells	12,8	28,8	05:35:37
4	bran	4,7	22,2	06:03:09
5	compost screening	8,3	41,6	01:37:00
10	wood chips from broadleaf forestry sites	5,7	30,6	05:10:55

3.1.3 Pilot-scale Pyrolysis

The experimental setup

The pilot-scale pyrolysis test was conducted using a dual auger pyrolysis plant made by REW Regenis. The plant is installed at our research facility in Wieselburg, Austria and has a nominal capacity of 20 kg/h biochar output.

The pyrolysis plant consists of the following functional component groups:

- Biomass input system
- Pyrolysis reactor
- Pyrolysis gas burner
- Flue gas scrubber
- Biochar output system

The feed dosing system, which consists of a mixing hopper having a volume of 6 m^3 and a variable speed dosing screw, is installed in the technical center of BEST. It is mechanically decoupled from the feeding screw and mounted on a scale which allows to measure the biomass feeding rate continuously.

The pyrolysis reactor, gas burner and flue gas system are installed in a 40' high cube container which is located outside, next to the technical center. The pyrolysis reactor consists of a 6 m long double walled double screw allotherm reactor. On one side biomass enters the reactor through the containers roof passing a double knife gate valve to prevent air passing into it. On the other side biochar exits and pyrolysis gases are extracted.

The biochar leaves the reactor also via a double knife gate valve, to prevent oxygen contamination of the pyrolysis zone. Then it is cooled by air in a double wall auger to ambient temperature and transported to storage vessels.

The gases are cleaned by a cyclone before they enter the gas burner. All parts of the gas section are heated to prevent tar condensation inside the pipes. The gas burner is specially designed for operation with pyrolysis gases, the gas mixed with preheated air and burned with

low emissions. A lambda probe continuously checks the excess air ratio and varies air flow rate. The combustion chamber is equipped with an additional liquid gas burner to heat it up to the working temperature.
The reactor is countercurrent heated by flue gases. Directly after the burning chamber the hot flue gases are diluted with cold air to the desired temperature for the pyrolysis process in the range of 300 to 800 °C and then the gases stream through the outer shelf of the reactors double wall. Two additional air injection points are also available to set the temperature along the reaction chamber to predefined temperatures.
Afterwards the flue gases are guided to the flue gas scrubber, where the gas is quenched and cleaned using water. Heat for additional purposes can be extracted from this water circuit or the temperature of this cycle is controlled using an external dry cooler.
The pyrolysis plant operates automatically, only the biochar hopper has to be emptied manually.

Figure 7: left: Pilot Scale pyrolysis plant from outside; right: pyrolysis plant inside container, pyrolysis reactor on left and gas burner on right side

Conducting the experiments

A pyrolysis experiment on pilot plant with sample 3 was performed over 5 days in the first half of September 2023. Continuous operation of the plant was not possible because of multiple problems associated with the level sensor on the end of the pyrolysis reactor. Mostly the fault stopped operation after 6 hours, thus measurement was split into multiple parts.
The pyrolysis parameters were similar to the tests performed with the lab-scale plant. Because of countercurrent heating the temperature inside the reactor is not constant. So, section 1 of the plant, which is the region near the biochar exit, has the highest temperature. The material temperature of pyrolysis in this section reached approximately 530 °C. It was almost stable during the test. Temperature in the other zones of the reactor still increased during tests, but this does not influence the quality of the pyrolysis product.

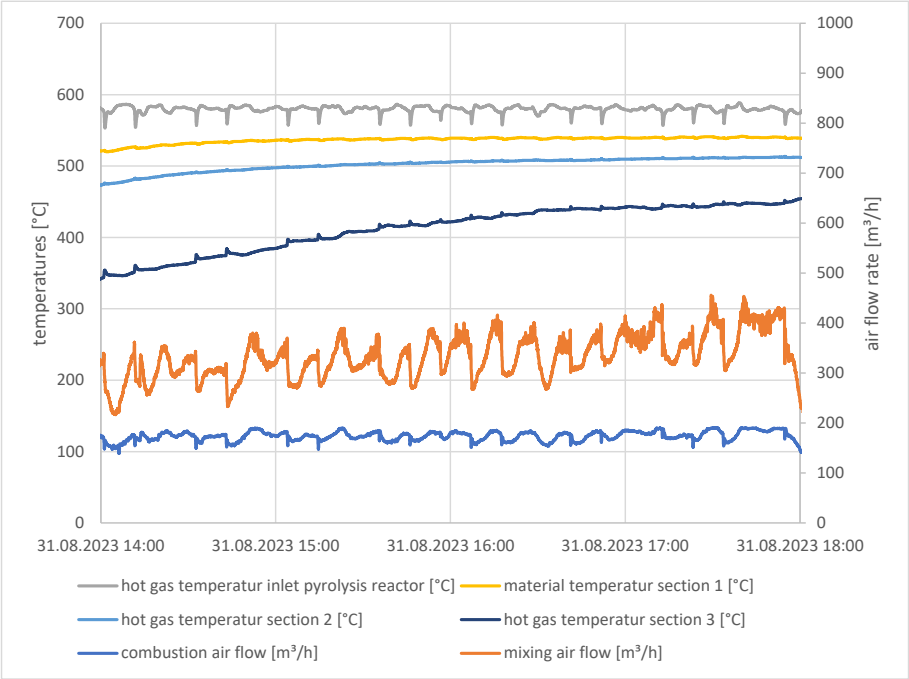

Figure 8: Course of temperature and air gas streams during pyrolysis test with walnut shells

The average residence time of the material inside the pyrolysis reactor was around 21 minutes, the average feed input rate was set to 49.5 kg/h.
An amount of 1221 kg of walnut shells, having a water content of 10.5 % was pyrolyzed during these tests and 249 kg of dry biochar were collected. Referring to dry input material, a biochar yield of 22.8 % was achieved.

3.2 Gasification

3.2.1 Sample Pretreatment

Chipping and sieving

The collected residues were separately chipped and were then sorted, using a test sieving machine with meshes of aperture sizes 8 and 3.15 mm, and the bottom plate. Some of the samples were dried at 105 °C in an oven for approximately 10 hours to have moisture levels in the 4-14% range that is suitable for gasification. The chipping machine used was the Tritone Maxi model manufactured by Ceccato Olindo s.r.l. (Figure: 9).

Figure: 9 Chipping machine (Tritone Maxi by Ceccato Olindo s.r.l.)

Figure 10: Test sieve machine (Titan 450 by Endecotts Ltd.)

Depending on the particle size, some of the collected samples were initially chipped using the chipping machine. The chipped output was then collected and sorted according to different size fractions using the Titan 450 test sieve machine manufactured by Endecotts Ltd. (Figure 10). The material collected on the sieve with mesh size 3.15 mm and the bottom plate was the usable material while that collected on the sieve of 8 mm aperture had to be re-chipped. In some cases, with very high fine dust-like particles, the material collected on the bottom plate had to be completely discarded as they would cause tight packing of the gasifier bed obstructing the flow of air through the reactor. Furthermore, a size index was assigned depending on visual inspection of the bulk of the particles: index 1 was assigned to residues with particle size lower than 1 cm, index 2 to residues with particle size between 1 and 3 cm, and index 3 to residues with particle size higher than 3 cm. Table 10 shows the pretreatment done for each of the residues in order of decreasing particle size:

Table 10: Pretreatment of the used residues

Code	Residue	Drying	Chipping	Sieving	Size index
7	wood affected by bark beetles	No	No	Yes	3
2	river woody debris	Yes	No	Yes	3
8	chestnut wood without tanins	Yes	No	Yes	2
9	vine prunings	No	Yes	Yes	1
6	spelt husks	No	No	Yes	1

3.2.2 Lab-scale Gasification

The experimental setup

The experiments on a lab-scale gasifier were conducted on a reverse updraft batch reactor at the Free University of Bozen-Bolzano, Italy. Figure 11 and Figure 12 show a schematic of the lab-scale set up and pictures during its operation, respectively. It includes a vertically installed reactor with a gas burner at the top end. It is mounted on a digital weighing scale; thus, the mass changes can be continuously monitored. In this reactor configuration, the flame propagates downward (opposite to the direction of air flow) as biomass is consumed. The

resulting producer gas flows upward through the drying, pyrolysis, and reduction zones, characterized by low tar content. The gas is drawn from the reactor and passed through a gas cleaning unit and then dried before being analyzed using a micro gas chromatograph (µGC 490, Agilent Technologies). Key components measured include CO, CO_2, H_2, CH_4, and N_2. However, in the present study the focus is on the biochar output from the reactor.

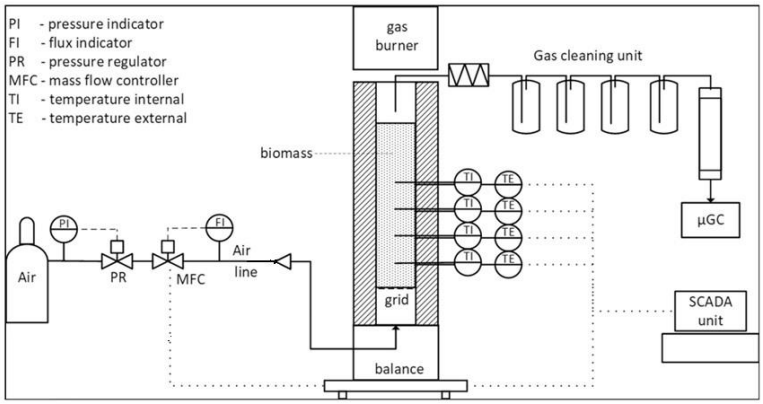

Figure 11: Schematic of lab-scale gasification system

Figure 12: Lab-scale gasifier – mounted on weighing scale (L), during operation (R)

The reactor comprises a cylindrical stainless-steel vessel, measuring 60 mm in diameter and 1300 mm in length. To minimize heat losses, thermal insulation is provided by a layer of glass wool with aluminum cladding. The residue is loaded from the upper part of the reactor and is retained by a distributor plate grate positioned 100 mm above the bottom. Each charge establishes a biomass bed at approximately 960 mm height. In this study, air serves as the gasification agent and is introduced from the bottom using two electronic mass flow controllers to control and maintain selected flow rates.

The experimental setup records biomass mass variation and air's mass flow rates. The experimental progress is marked by the propagation of the flaming pyrolysis zone across the reactor, consuming biomass and producing biochar, measured by the temperatures at the various thermocouples installed along its length. The unique feature of this configuration lies in placing the reactor on a digital weighing scale, allowing real-time monitoring of biomass mass loss during each test. This innovative setup takes advantage of downdraft gasifier benefits, particularly the cracking of tars on the biochar bed.

Experimental findings

The experiments were conducted on the lab-scale setup to assess biochar production and its characteristics. All the five residues mentioned above, Wood affected by bark beetles (BW), river woody debris (RW), chestnut wood without tannins (CN), vine prunings (VP), and spelt husks (SH), were tested under operating conditions that allowed a biochar yield of about 20%. The temperatures and the biochar yields were analyzed as a function of residue diameter and moisture. From the experiments, it was observed that particle size, indicated by the size index, and the maximum temperatures attained during the test, play an important role in the gasification process. Moreover, the moisture content of the residue also influences the overall biochar yield. The results are reported in the Table 11.

Table 11: The moisture content and maximum temperature attained for the various residue and the biochar yield

Code	Residue	Moisture content in w/w %	T_{max} in °C	Biochar yield in w/w % $_{w.b.}$
7	Wood affected by bark beetles - BW	4.38	550	21.5
8	Chestnut wood without tanins - CN	10.53	639	20.1
9	Vine prunings - VP	13.01	760	18.3
6	Spelt husks - SH	8.86	775	18.7
2	River woody debris - RW	7.46	502	22.4

The mass fraction of the biochar produced, or biochar yield, has a strong positive correlation with the size index of the residue and a negative correlation with the maximum temperature of the process (Figure 13.a and b). It was found to have a generally negative correlation with the moisture content of the residue (Figure 13.c). The biochar yield in all samples was in the range of 18-23% on a wet basis (w.b.). The maximum temperatures in all experiments were in the range of 500-800 °C, with the smaller size index samples (VP and SH) reaching the highest temperatures (Table 11). At temperatures higher than 650 °C, biochar is thermally stable and becomes more hydrophobic (Ghani *et al.*, 2013). However, the mass fraction of biochar yield was low in these cases, with an average yield below 19%.

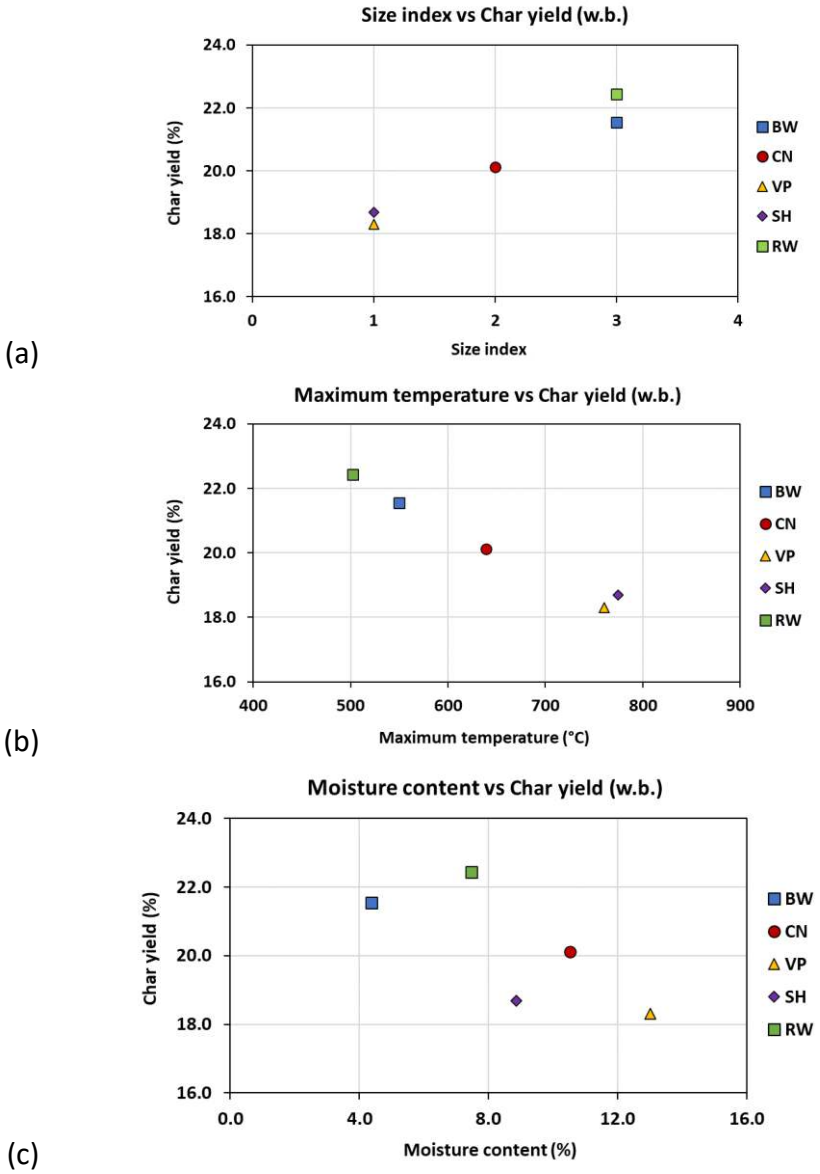

Figure 13: Mass fraction of biochar (%) as a function of: (a) Size index, (b) Maximum temperature, (c) Moisture content.

Further, the interaction effects between the moisture content and the maximum temperatures obtained for the different residues are shown in Figure 14.a. As the moisture content in the residue increases the maximum temperature that can be achieved also increases (Table 11). The moisture content for all the residues were below 11% except in the case of VP, which was about 13%. As mentioned, VP, along with SH, were the two residues that yielded the lowest relative amount of biochar, while those with low moisture content (BW and RW) yielded the highest biochar content (over 21%). It is also worth noting that the larger-size particle residues were drier than the small-size index residues (Figure 14.b). The high temperatures achieved in the smaller size index residues (Figure 14.c) could be possibly due to the faster burnout of the smaller particles when compared to those with larger size indexes.

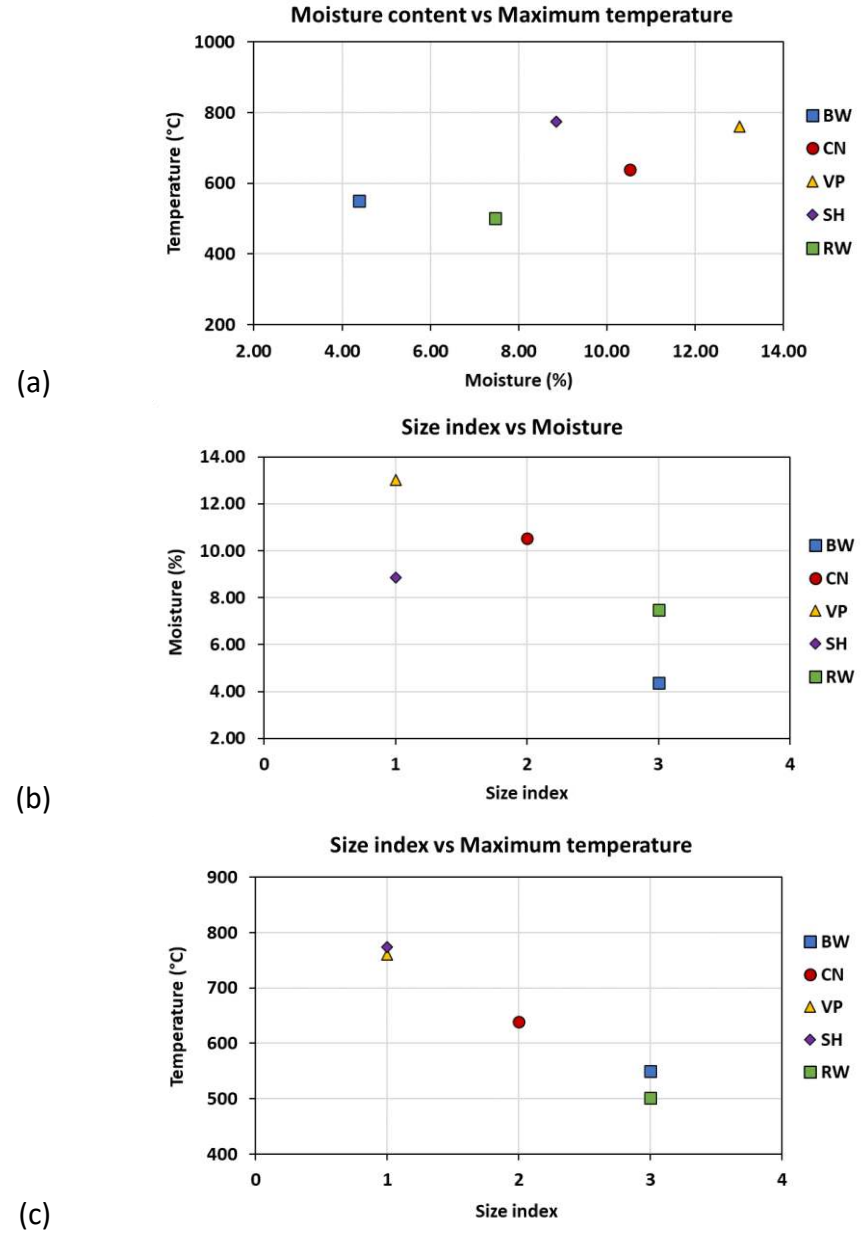

Figure 14: Interaction effects between residue moisture content (a), particle size (b), and maximum temperatures (c) achieved during gasification.

Table 12: Producer gas composition of the experiments conducted on the lab-scale gasifier.

Residue	H_2 in %	CO in %	CO_2 in %	N_2 in %	CH_4 in %	C_2H_6 in %
Wood affected by bark beetles - **BW**	1.98±0.19	13.91±0.40	19.34±1.15	62.16±1.24	2.35±0.26	0.25±0.02
River woody debris - **RW**	1.99±0.43	11.67±1.04	18.98±4.96	65.29±4.76	1.88±0.38	0.20±0.03
Chestnut wood without tanins - **CN**	2.16±0.17	13.98±0.66	16.90±0.26	65.02±0.97	1.78±0.17	0.16±0.01
Vine prunings - **VP**	9.46±0.30	11.13±0.33	19.58±0.72	57.07±0.88	2.53±0.08	0.23±0.03
Spelt husks - **SH**	4.13±0.17	20.65±0.74	11.41±1.40	61.25±0.49	2.39±0.14	0.18±0.02

Regarding the gas composition (Table 12), it was observed that the high temperatures of VP and SH lead to high fractions of H_2 (9.5%) and CO (20.6%) respectively. These values are comparable to values in syngas obtained from air gasification of biomass (Couto *et al.*, 2013; Maschio *et al.*, 1994). For all the other residues, H_2 was in the range 1.9% - 2.2% while CO was in the range 11.7% - 14.0%.

Mass and energy balance

As previously mentioned, the biomass consumption rate is measured using the digital weighing scale while the gasifying agent (air) is supplied in a controlled manner and at a known rate using mass flow controllers. The mass balances of the different runs were calculated using the following formula:

$$\dot{m}_{biomass} + \dot{m}_{air} = \dot{m}_{char} + (\dot{m}_{PG\_dry} + \dot{m}_{condensate})$$

where $\dot{m}_{biomass}$ is the mass flow rate of the biomass fed to the reactor, $\dot{m}_{air}$ is the mass flow rate of the air supplied to the system, $\dot{m}_{char}$ is the mass flow rate of the biochar produced during the test, $\dot{m}_{PG\_dry}$ is the mass flow rate of dry producer gas (PG) and $\dot{m}_{condensate}$ is the mass flow rate of the condensate exiting the reactor. The results are tabulated in Table 13.

Table 13: Mass balances of the experiments conducted on the lab-scale gasifier

Code	Residue	Input		Output	
		Biomass w.b. in kg/h	Air in kg/h	Biochar d.b. in kg/h	PG d.b. + Condensate in kg/h
7	wood affected by bark beetles - **BW**	1.20	0.73	0.26	1.67
8	chestnut wood without tanins - **CN**	1.02	0.79	0.20	1.60
9	vine prunings - **VP**	0.96	0.98	0.18	1.77
6	spelt husks - **SH**	0.65	0.81	0.12	1.34
2	river woody debris - **RW**	1.13	0.69	0.25	1.57

Similarly, the energy balance of the system was computed using the formula:

$$\dot{E}_{biomass} = \dot{E}_{char} + (\dot{E}_{PG_{dry}} + \dot{E}_{condensate} + \dot{E}_{losses})$$

where $\dot{E}_{biomass}$ is the energy associated with the biomass flowing into the reactor, $\dot{E}_{char}$ is the energy associated with the flow rate of biochar produced during the test, $\dot{E}_{PG\_dry}$ is the energy associated with the flow rate of dry PG, $\dot{E}_{condensate}$ is the energy associated with the condensate exiting the reactor, and $\dot{E}_{losses}$ is the energy lost from the gasifier during operation. Results are shown in Table 14.

Table 14: Energy balances of the experiments conducted on the lab-scale gasifier considering 1h of continuous operation.

Code	Residue	Input	Output	
		$Biomass_{d.b.}$ in kWh	**$Biochar_{d.b.}$ in kWh**	**$PG_{d.b.}$ + Condensate + Losses in kWh**
7	wood affected by bark beetles - **BW**	6.12	2.15	3.96
8	chestnut wood without tanins - **CN**	4.69	1.71	2.98
9	vine prunings - **VP**	4.25	1.42	2.83
6	spelt husks - **SH**	2.77	0.67	2.10
2	river woody debris - **RW**	5.20	1.95	3.25

3.2.3 Pilot-scale Gasification

Experimental setup

The experiments were conducted on the pilot-scale gasification system, the schematic of which is shown in Figure 15 and a picture in Figure 16. It comprises a feedstock loading tank in which biomass of appropriate particle size is loaded. This residue is then loaded into the reactor from the bottom, in a controlled manner, using a vertical loading system. The reactor furnace is equipped with thermocouples, at various points along its length, to monitor the temperatures during operation. The temperatures indicate the position and the propagation of the combustion zone in the reactor. The gasifying agent, air in this case, is also supplied through a nozzle at the lower portion of the reactor and flows upwards, thus making it of co-current configuration. Both the producer gas and the biochar exit from the top of the reactor. A small fraction of the producer gas is sent to a micro gas chromatograph (µGC 490, Agilent Technologies) to quantify the gas components, and the remainder is burned in a flare to prevent the escape of any harmful gases. The biochar is collected in a biochar tank and its mass can continuously be monitored.

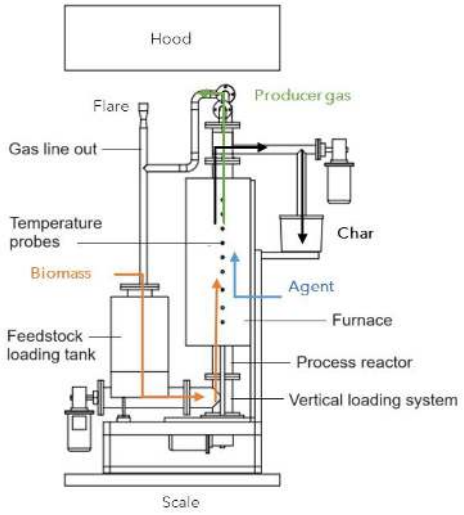

Figure 15: Schematic of pilot scale gasification system

Figure 16: Pilot scale gasification setup

Experimental findings

The BW residue was chosen for pilot-scale tests. Six tests were conducted over six different days. The first two tests of duration approximately four hours each, were conducted as preliminary tests to ensure the correct operation of the system. The final four tests were all conducted at a constant airflow rate of 21 NLPM. The details are tabulated in Table 15: Pilot-scale gasification tests on wood affected by bark beetles (BW). The average biochar yield [d.b.] of the four main experimental runs during steady-state operation was 19.0±0.6 %.

Table 15: Pilot-scale gasification tests on wood affected by bark beetles (BW)

	Preliminary tests		**Main tests**			
	Test - 1	**Test - 2**	**Test – 3**	**Test - 4**	**Test - 5**	**Test - 6**
Residue moisture in w/w %	8.11	9.14	9.14	8.77	9.12	9.46
Test duration in h						
Warm-up time	0.69	1.07	0.60	0.70	0.75	0.66
Steady-state time	3.13	3.15	3.90	5.73	5.22	5.17
Total time	3.82	4.22	4.50	6.43	5.97	5.83
Biomass consumed in kg						
Warm-up	0.5	0.5	0.5	0.5	0.5	0.5
Steady-state	5.5	8.5	8.1	11.8	10.8	10.4
Total	6.0	9.0	8.6	12.3	11.3	10.9
Biomass flow rate in kg/h						
Steady-state	1.91	2.86	2.08	2.06	2.07	2.01
Total	1.44	2.02	1.91	1.91	1.89	1.87
Biochar yield$_{d.b.}$ in kg						
Total	1	1	1.6	2.3	2	1.9
Biochar yield in %						
Steady-state	16.7	11.1	19.8	19.5	18.5	18.3
Total	18.2	11.8	18.6	18.7	17.7	17.4

The gas compositions obtained during the four main tests are reported in Table 16. The results obtained proved the good repeatability of the tests.

Table 16: Average gas composition of the four main tests

Experiment	**H_2**	**N_2**	**CH_4**	**CO**	**CO_2**	**C_2H_6**
Test – 3	13.7±3.2	47.9±3.6	3.6±0.6	16.4±1.4	18.1±1.0	0.31±0.05
Test – 4	14.8±2.0	47.3±1.8	3.7±0.3	16.2±0.4	17.7±0.4	0.29±0.02
Test – 5	12.7±1.4	50.0±1.2	3.5±0.1	15.9±0.4	17.7±0.5	0.28±0.01
Test – 6	12.5±1.7	50.2±1.6	3.6±0.2	15.7±0.5	17.9±0.4	0.29±0.01

A clear difference is evident in the gas composition of the pilot-scale tests when compared to that of the lab-scale, especially for the major combustible components H_2 and CO. The average H_2 content was about seven times higher in the case of the pilot-scale tests, and CO was about 2% higher. On the other hand, the average N_2 concentration was about 13% lower in the pilot-scale tests as compared to the lab-scale test on BW.

Moreover, the effect of temperature on the overall biochar yield is evident (see Table 11). In the case of Test – 3 and Test – 4 the average temperatures are higher at the middle region of the reactor, and lower at the top, when compared to Test – 5 and Test – 6, indicating a hotter biochar bed located more towards the mid-section. In such an operation, the biochar yield was found to be higher, and so were the combustible components H_2 and CO in the PG. This could possibly be due to a larger reduction zone at the top of the reactor near the gas exit.

Table 17: Average temperatures recorded at various points along the pilot-scale reactor shown in Figure 17.

Experiment	Biomass IN	Bottom	Middle	Top	Ext-Mid	Ext-Top	Gas OUT
Test - 3	27.6±2.8	49.9±24.0	125.9±47.0	264.2±49.0	162.5±55.4	358.0±54.5	165.6±28.8
Test - 4	22.9±1.0	37.6±3.1	109.0±24.4	287.2±50.3	138.3±23.1	400.0±28.7	179.6±23.5
Test - 5	23.7±1.6	35.5±2.0	**98.8±17.0**	**323.9±34.1**	133.9±17.0	**441.9±34.2**	**195.7±18.4**
Test - 6	24.7±2.1	39.6±10.6	**93.5±14.1**	**305.2±47.9**	136.0±20.8	**442.4±50.3**	**192.4±27.8**

Figure 17: Locations of the various temperature measurement points along the reactor

Mass and energy balance

The mass and energy balances were performed using the same equations as for the lab-scale plant. The mass balances for all tests are provided in Table 18. The energy balances for one preliminary and one experimental test are provided in Table 19. As the air injected is increased, the biomass consumption rate also increases. This is expected as the higher air

inflow would cause faster particle burnout in the reactor bed. However, it was observed that even with the higher flow rate, there were differences in the biochar yield fraction for the four different runs. The maximum biochar yield [d.b] of 19.8% was recorded at a biomass flow rate of 2.08 kg/h and an air flow rate of 1.48 kg/h.

Table 18: Mass balances of the experiments conducted on the pilot-scale gasifier.

Experiment	Input		Output	
	Biomass $_{w.b.}$ in kg/h	**Air in kg/h**	**Biochar $_{d.b.}$ in kg/h**	**$PG_{d.b.}$ + Condensate in kg/h**
Test – 1	1.91	1.41	0.32	3.01
Test – 5	2.07	1.49	0.38	3.18

Table 19: Energy balances of the experiments conducted on the pilot-scale gasifier considering 1h of continuous operation.

Experiment	Input	Output	
	Biomass $_{d.b.}$ in kWh	**Biochar $_{d.b.}$ in kWh**	**$PG_{d.b.}$ + Condensate + Losses in kWh**
Test – 1	10.28	2.65	7.62
Test – 5	11.14	3.22	7.92

4 Biochar Characterization

4.1 Results and Discussion

The biochar samples were characterized at the National Institute of Chemistry (NIC), at Free University of Bozen-Bolzano (unibz – Bioenergy and Biofuels Laboratories) and at the Water & Life Lab srl. The list of samples is presented in Table 20.
Biochar characterizations performed at Water & Life Lab srl were elemental composition, other biochar properties (e.g. water holding capacity), PAH and PCB & PCDD/PCDF.
Biochar characterizations performed at unibz were: elemental analyses (C, H, N, S), moisture and ash content. Moreover, the higher heating value was calculated according to the Milne's formula. Biochar characterizations performed at NIC were: X-ray Powder Diffraction (XRD), Thermogravimetry (TG), pH measurements, Scanning Electron Microscopy (SEM) and ATR-FTIR spectroscopy.

Table 20: List of the biochar samples. BC stands for biochar; PL stands for pyrolysis labscale; GL stands for gasification labscale; PP stands for pyrolysis pilotscale; GP stands for gasification pilotscale;

Biochar Code	Residue	Residue abbreviation	Production process
1.BC.PL	coffee husks		pyrolysis - lab
2.BC.GL	River woody debris	RW	gasification - lab
3.BC.PL	walnut shells		pyrolysis - lab
4.BC.PL	bran		pyrolysis - lab
5.BC.PL	Compost screenings		pyrolysis - lab
6.BC.GL	spelt husks	SH	gasification - lab
7.BC.GL	wood affected by bark beetles		gasification - lab
8.BC.GL	Chestnut wood without tannins	CN	gasification - lab
9.BC.GL	Vine prunings	VP	gasification - lab
10.BC.PL	wood chips from broadleaf forestry sites		pyrolysis - lab
7.BC.GP	wood affected by bark beetles	BW	gasification - pilot
3.BC.PP	walnut shells		pyrolysis - pilot

4.1.1 Basic Characterization

The Results from the basic characterization done by unibz are shown in Table 21. The ash content varied considerably between the samples with the maximum ash content being 39.68 w/w % $_{d.b.}$ in sample 6.BC.GL and the minimum ash content being 1.17 w/w % $_{d.b.}$ in sample 8.BC.GL. The average ash content for the pyrolysis samples was 15.06±10.97 and for the gasification samples 11.13±13.50 w/w % $_{d.b.}$. The carbon content had its maximum value in sample 7.BC.GP with 87.21 w/w % $_{d.b.}$ and its minimum value in sample 5.BC.PL with 49.02 w/w% $_{d.b.}$. The average carbon content for the pyrolysis samples was 69.13±12.39 and for the gasification samples 78.25±9.96 w/w % $_{d.b.}$. The hydrogen content had its maximum value in sample 1.BC.PL with 3.31 w/w % $_{d.b.}$ and its minimum value in sample 6.BC.GL with 0.89 w/w

% $_{d.b.}$. The average hydrogen content for the pyrolysis samples was 2.69±0.54 and for the gasification samples 2.07±0.92 w/w % $_{d.b.}$. The nitrogen content had its maximum value in sample 4.BC.PL with 3.92 w/w % $_{d.b.}$ and its minimum value in sample 7.BC.GL with 0.41 w/w % $_{d.b.}$. The average nitrogen content for the pyrolysis samples was 2.13±1.25 and for the gasification samples 0.62±0.26 w/w % $_{d.b.}$ The sulfur content had its maximum in sample 1.BC.PL with 0.55 w/w % $_{d.b.}$ and its minimum value in samples 6.BC.GL, 7.BC.GL and 8.GC.GL with 0.09 w/w % $_{d.b.}$. The average sulfur content for the pyrolysis samples was 0.34±0.10 and for the gasification samples 0.14±0.08 w/w % $_{d.b.}$. The oxygen content had its maximum value in sample 2.BC.GL with 14.86 w/w % $_{d.b.}$ and its minimum value in sample 9.BC.GL with 0.74 w/w % d.b. The average oxygen content for the pyrolysis sample was 10.11±2.49 and for the gasification samples 7.80±5.23 w/w % $_{d.b.}$. The higher heating value had its maximum value in sample 3.BC.PP with 32.26 MJ/kg $_{d.b.}$ and its minimum value in sample 5.BC.PL with 16.98 MJ/kg $_{d.b.}$. The average higher heating value for the pyrolysis samples was 25.44±5.11 and for the gasification samples 28.25±3.85 MJ/kg $_{d.b.}$.

Table 21: The results from the analyses done by unibz

Biochar Code	Ash	C	H	N	S	O	HHV_{Milne}	LHV_{Milne}
	w/w % $_{d.b.}$						MJ/kg $_{d.b.}$	
6.BC.GL	39.68	57.16	0.89	0.45	0.09	1.73	19.81	19.62
7.BC.GL	2.76	81.72	3.25	0.41	0.09	11.77	30.67	29.96
9.BC.GL	14.75	81.51	1.55	1.16	0.29	0.74	29.41	29.07
8.BC.GL	1.17	84.97	2.32	0.44	0.09	11.02	30.65	30.15
2.BC.GL	4.25	76.92	3.19	0.69	0.10	14.86	28.52	27.83
4.BC.PL	23.79	62.19	1.96	3.92	0.29	7.85	22.04	21.61
5.BC.PL	33.14	49.02	1.98	2.23	0.35	13.29	16.98	16.55
10.BC.PL	9.25	73.21	2.88	0.98	0.25	13.43	26.92	26.29
3.BC.PL	3.75	81.90	2.80	1.16	0.25	10.14	30.24	29.63
1.BC.PL	20.19	63.36	3.31	3.62	0.55	8.97	24.20	23.48
7.BC.GP	4.17	87.21	1.23	0.56	0.18	6.67	30.44	30.17
3.BC.PP	3.51	85.10	3.19	0.86	0.33	7.01	32.26	31.56

Looking at elemental content, it becomes clear that all of the samples seem suitable for agricultural application from their major elemental composition. For agricultural application, the EBC requires a molar H/C_{org} ratio of below 0.7 (for feed additive certification even <0.4). Additionally, the O/C_{org} ratio needs to be <0.4. As can be seen in Table 22, all of the biochar samples have a H/C_{total} <0.7 and in the case of the samples 6.BC.GL, 9.BC.GL, 8.GC.GL and 7.BC.GP even <0.4. The O/C_{total} ratio is below 0.4 for all samples. Although the EBC requires C_{org} to be determined, which excludes Carbonates, for this project it was assumed that C_{total}~C_{org} as biochar usually contains very little carbonates (Wang *et al.,* 2014). Another interesting aspect regarding potential application of the produced biochars are their high heating values. With higher heating values averaging ~25 and ~28 MJ/kg $_{d.b.}$ for pyrolysis and gasification respectively, they are near or above the required >27 MJ/kg $_{d.b.}$ to replace coke in

steel production, according to Safarian (Safarian, 2023). Looking at individual samples, the samples 7.BC.GL, 9.BC.GL, 8.BC.GL, 2.BC.GL, 3.BC.PL, 7.BC.GP and 3.BC.PP fulfill this requirement. In addition to that, all of these samples except 9.BC.GL show ash values <10 w/w % $_{d.b.}$, which is also a requirement for the application in certain steel making processes according to Quicker an Weber (Quicker and Weber, 2016).

Table 22: H/C molar and O/C molar ratios for each sample

Sample Code	H/C molar	O/C molar
6.BC.GL	0.19	0.02
7.BC.GL	0.47	0.11
9.BC.GL	0.23	0.01
8.BC.GL	0.33	0.10
2.BC.GL	0.49	0.15
4.BC.PL	0.38	0.09
5.BC.PL	0.48	0.20
10.BC.PL	0.47	0.14
3.BC.PL	0.41	0.09
1.BC.PL	0.62	0.11
7.BC.GP	0.17	0.06
3.BC.PP	0.45	0.06

4.1.2 Elemental Composition

The elemental composition was determined by Water & Life lab according to the methods for elemental composition ISO 54321:2021 Met B and EN 16170:2016. Results are presented in Table 23. Arsenic was only detected in sample 5.BC.PL with a value of 1.8 mg/kg $_{d.b.}$. Cadmium was only detected in sample 2.BC.GL with a value of 0.6 mg/kg $_{d.b.}$. Mercury was detected in no sample. Thallium was detected in no sample. Vanadium was only detected in samples 5.BC.PL with 16.6 mg/kg $_{d.b.}$ and sample 2.BC.GL with 3.2 mg/kg $_{d.b.}$. Lead was only detected in samples 2.BC.GL, 6.BC.GL, 8.BC.GL, 5.BC.PL and 10.BC.PL, with the highest amount being 10.2 mg/kg $_{d.b.}$ in 5.BC.PL. Molybdenum was only detected in samples 6.BC.GL, 4.BC.PL, 5.BC.PL and 10.BC.PL, with the highest amount being 5.9 mg/kg $_{d.b.}$ in 5.BC.PL. Chromium was detected in every sample, with a maximum of 65.7 mg/kg $_{d.b.}$ in sample 2.BC.GL and a minimum of 0.5 mg/kg $_{d.b.}$. in sample 7.BC.GL. The average chromium content for the pyrolysis samples was 13.4±13.3 and for the gasification samples 20.3±22.0 mg/kg $_{d.b.}$. Manganese was found to be highest in sample 5.BC.PL with 349.6 mg/kg $_{d.b.}$ and lowest in sample 3.BC.PP with 9.0 mg/kg $_{d.b.}$. The average manganese content for the pyrolysis samples was 146.1±146.8 and for the gasification samples 124.4±48.8 mg/kg $_{d.b.}$. Nickel was found to be highest in sample 5.BC.PL with 22.7 mg/kg $_{d.b.}$ and lowest in sample 7.BC.GL with <0.5 mg/kg $_{d.b.}$. The average nickel content for the pyrolysis samples was 7.9±6.8 and for the gasification samples 6.0±3.4 mg/kg $_{d.b.}$. Copper was found to be highest in the sample 1.BC.PL with 136.0 mg/kg $_{d.b.}$ and lowest in the sample 6.BC.GL with 2.2 mg/kg $_{d.b.}$. The average copper content for the pyrolysis samples was 37.9±45.2 and for the gasification samples 13.5±16.6 mg/kg $_{d.b.}$. Zinc was found to be highest in the sample 4.BC.PL with 298.8 mg/kg $_{d.b.}$ and lowest in the sample 3.BC.PP with 7.5 mg/kg $_{d.b.}$. The average zinc content for the pyrolysis samples was 94.9±99.6 and for

the gasification samples 49.3±34.5 mg/kg $_{d.b.}$. Phosphorous was found to be highest in the sample 4.BC.PL with 49119.7 mg/kg $_{d.b.}$ and lowest in the sample 8.BC.GL with 48.4 mg/kg $_{d.b.}$. The average phosphorous content for the pyrolysis samples was 9736.1±17654 and for the gasification samples 1261.7±1608.4 mg/kg $_{d.b.}$. Potassium was found to be highest in the sample 1.BC.PL with 43193.7 mg/kg $_{d.b.}$ and lowest in the sample 8.BC.GL with 81.4 mg/kg $_{d.b.}$. The average potassium content for the pyrolysis samples was 21913.0±14761.2 and for the gasification samples 5901.7±7340.0 mg/kg $_{d.b.}$.

These often quite stark concentration differences between pyrolysis and gasification samples are most likely not technology related, but rather feedstock based. These non-volatile elements are present in different concentrations in the respective residues and are hardly affected by the process(Ippolito *et al.*, 2020). From an agricultural standpoint most of the chars are completely in line with even the lowest EBC-thresholds (EBC, 2023). Only samples 1.BC.PL and 4.BC.PL violate some of the thresholds. For sample 1.BC.PL the Copper content of 136.0 mg/kg $_{d.b.}$ is way above the required <100 mg/kg $_{d.b.}$ for the agricultural certificates. According to the EBC, it may only be used as a basic resource. For sample 4.BC.PL the Zinc content of 298.8 mg/kg $_{d.b.}$ is way above the required <200 mg/kg $_{d.b.}$ for the organic agriculture certificate. It may, however, still be suitable for regular agriculture. What can be a great asset regarding agricultural application for some of the analysed samples is their high nutrient content. As the most effective application of biochar in agriculture is in combination with some fertilizing agent(Bai *et al.*, 2020), the more nutrient the chars contain on themselves, the less fertilizing agent will be necessary, assuming a high bioavailability of the nutrients in the biochar. In that sense, samples like 4.BC.PL or 1.BC.PL are clearly preferred over samples like 8.BC.GL or 2.BC.GL.

Table 23: Elemental composition of the biochar gasification samples made river woody debris - 2.BC.GL; spelt husks - 6.BC.GL; wood affected by bark beetles - 7.BC.GL; chestnut wood without tannins - 8.BC.GL; vine prunings - 9.BC.GL; wood affected by bark beetles - 7.BC.GP; and the biochar pyrolysis samples made from coffee husks - 1.BC.PL ; walnut shells - 3.BC.PL; bran 4.BC.PL; Compost screenings - 5.BC.PL; wood chips from broadleaf forestry sites - 10.BC.PL; walnut shells - 3.BC.PP WS; BC stands for biochar; PL stands for pyrolysis labscale; GL stands for gasification labscale; PP stands for pyrolysis pilotscale; GP stands for gasification pilotscale;

	2.BC.GL	**6.BC.GL**	**7.BC.GL**	**8.BC.GL**	**9.BC.GL**	**7.BC.GP**	**1.BC.PL**	**3.BC.PL**	**4.BC.PL**	**5.BC.PL**	**10.BC.PL**	**3.BC.PP**
	mg/kg d.b.	**mg/kg d.b.**	**mg/kg d.b.**	**mg/kg d.b.**	**mg/kg d.b.**	**mg/kg d.b.**	**mg/kg d.b.**	**mg/kg d.b.**	**mg/kg d.b.**	**mg/kg d.b.**	**mg/kg d.b.**	**mg/kg d.b.**
Arsenic	< 1.0	< 1.0	< 1.0	< 1.0	< 1.0	< 1.0	< 1.0	< 1.0	< 1.0	1.8	< 1.0	< 1.0
Cadmium	0.6	< 0.5	< 0.5	< 0.5	< 0.5	< 0.5	< 0.5	< 0.5	< 0.5	< 0.5	< 0.5	< 0.5
Total chromium	65.7	16.4	0.5	2.0	11.3	25.9	8.7	6.3	11.4	42.8	6.4	4.8
Phosphorus	587.1	2 179.9	162.6	48.4	4 464.4	127.5	1 863.2	810.6	49 119.7	4 308.9	1 782.6	531.5
Manganese	201.6	87.3	170.8	112.0	118.1	56.6	127.2	16.4	334.3	349.6	40.1	9.0
Mercury	< 0.01	< 0.01	< 0.01	< 0.01	< 0.01	< 0.01	< 0.01	< 0.01	< 0.01	< 0.01	< 0.01	< 0.01
Molybdenum	< 0.5	0.7	< 0.5	< 0.5	< 0.5	< 0.5	< 0.5	< 0.5	5.1	5.9	0.7	< 0.5
Nickel	3.1	7.7	< 0.5	2.1	5.5	11.6	6.0	3.9	8.2	22.7	3.8	2.9
Lead	5.1	0.8	< 0.5	0.7	< 0.5	< 0.5	< 0.5	< 0.5	< 0.5	10.2	1.1	< 0.5
Potassium	1 010.9	7 299.6	2 714.7	81.4	21 511.8	2 791.9	43 193.7	8 810.4	37 190.5	27 388.8	8 120.6	6 774.1
Copper	46.6	2.2	2.7	3.5	23.5	2.6	136.0	6.1	28.5	35.1	15.8	5.6
Thallium	< 0.5	< 0.5	< 0.5	< 0.5	< 0.5	< 0.5	< 1	< 1	< 1	< 1	< 1	< 1
Vanadium	3.2	< 2.5	< 2.5	< 2.5	< 2.5	< 2.5	< 2.5	< 2.5	< 2.5	16.6	< 2.5	< 2.5
Zinc	68.9	20.5	48.7	8.5	113.2	36.1	44.5	10.4	298.8	118.2	90.0	7.5

4.1.3 Other Biochar Properties

Table 24: Other properties of the biochar gasification samples made river woody debris - 2.BC.GL; spelt husks - 6.BC.GL; wood affected by bark beetles - 7.BC.GL; chestnut wood without tannins - 8.BC.GL; vine prunings - 9.BC.GL; wood affected by bark beetles - 7.BC.GP; and the biochar pyrolysis samples made from coffee husks - 1.BC.PL ; walnut shells - 3.BC.PL; bran 4.BC.PL; Compost screenings - 5.BC.PL; wood chips from broadleaf forestry sites - 10.BC.PL; walnut shells - 3.BC.PP WS; BC stands for biochar; PL stands for pyrolysis labscale; GL stands for gasification labscale; PP stands for pyrolysis pilotscale; GP stands for gasification pilotscale;

		2.BC.GL	6.BC.GL	7.BC.GL	8.BC.GL	9.BC.GL	7.BC.GP	1.BC.PL	3.BC.PL	4.BC.PL	5.BC.PL	10.BC.PL	3.BC.PP
	unit												
Water holding capacity	g/g	4.8	6.0	5.3	3.9	3.4	2.6	3.8	1.9	2.9	2.2	2.4	2.0
Residual at 105°C	w/w %	99	98	98	98	97	100	89	87	96	91	92	99
moisture	w/w %	1	2	2	2	3	0	11	13	4	9	8	1
Cation exchange capacity with $BaCl_2$	meq/100g	25.0	18.8	25.2	16.2	19.0	20.3	24.5	13.9	16.3	24.3	23.6	17.6
Chlorides	mg/kg $_{d.b.}$	43	354	34	13	219	34	1 149	299	416	7 166	150	305

Results are presented in Table 24. The water holding capacity of the analysed samples ranged from 1.9 to 6.0, with the minimum being found in 3.BC.PL and the maximum being found in 6.BC.GL. The gasification samples seem to have a slightly higher water holding capacity than the pyrolysis samples with an average of 4.3±1.2 vs 2.5±0.7 g/g. The moisture content was the highest in the sample 3.BC.PL with 13 w/w% and lowest in the sample 7.BC.GP with 0 w/w%. The average for the pyrolysis samples was 8±4 and for the gasification samples 2±1 w/w%. The cation exchange capacity was the highest in the sample 7.BC.GL with 25.2 meq/100 g and lowest in the sample 3.BC.PL with 13.9 meq/100 g. The average for the pyrolysis samples was 20.0±4.2 and for the gasification samples 20.8±3.3 meq/100 g. These values are similar to reported ones in the literature and higher as a standard soil sample (Lee *et al.*, 2016) meaning that the chars could be used to improve the cation exchange capacity of certain soils. However, as the cation exchange capacity depends on the used method to determine it, one has to be cautious when comparing data directly (Munera-Echeverri *et al.*, 2018). The chlorides had their highest concentration in the sample 5.BC.PL with 7166 mg/kg and their lowest in the sample 8.BC.GL with 13 mg/kg. The average for the pyrolysis samples was 1581±2518 and for the gasification samples 116±126 mg/kg. These differences are most likely due to differences in feedstocks, as the feedstock determines the potential maximum concentration in the biochar (granted that no contamination or willful addition happens). For example, the highest chloride value in sample 5.BC.PL, which refers to the compost screening surplus residue, corresponds with the highest chlorine level in the residues (see Table 3). The used methods for determining the water holding capacity was

EN ISO 14238:2014 annex A; for determining the residual at 105°C were ISO 14820-2:2016 and CEN/TS 17773:2022; for determining moisture content were ISO 14820-2:2016 and CEN/TS 17773:2022; for determining cation exchange capacity with BaCl2 were D.M. 13/09/99 GU n°248 21/10/1999 Met.XIII.2 and DM 25/03/2002 GU 84 10/04/2002; and for chloride measurements CEN/TS 17758:2022;

4.1.4 PAH Measurements

Table 25: Sum of PAH and individual PAH results of the biochar gasification samples made river woody debris - 2.BC.GL; spelt husks - 6.BC.GL; wood affected by bark beetles - 7.BC.GL; chestnut wood without tannins - 8.BC.GL; vine prunings - 9.BC.GL; wood affected by bark beetles - 7.BC.GP; and the biochar pyrolysis samples made from coffee husks - 1.BC.PL ; walnut shells - 3.BC.PL; bran 4.BC.PL; Compost screenings - 5.BC.PL; wood chips from broadleaf forestry sites - 10.BC.PL; walnut shells - 3.BC.PP WS; BC stands for biochar; PL stands for pyrolysis labscale; GL stands for gasification labscale; PP stands for pyrolysis pilotscale; GP stands for gasification pilotscale

		2.BC.GL	6.BC.GL	7.BC.GL	8.BC.GL	9.BC.GL	7.BC.GP	1.BC.PL	3.BC.PL	4.BC.PL	5.BC.PL	10.BC.PL	3.BC.PP
Acenaphthene	mg/kg d.b.	< 0.01	< 0.01	< 0.01	< 0.01	< 0.01	0.90	0.50	0.32	0.07	0.40	0.11	< 0.01
Acenaphthylene	mg/kg d.b.	< 0.01	< 0.01	< 0.01	< 0.01	< 0.01	2.61	0.12	0.06	0.02	0.09	0.08	< 0.01
Anthracene	mg/kg d.b.	< 0.01	< 0.01	< 0.01	< 0.01	< 0.01	0.29	0.51	1.03	0.37	0.45	0.37	0.03
Benzo(a)anthracene	mg/kg d.b.	< 0.01	< 0.01	< 0.01	< 0.01	< 0.01	0.07	0.23	0.14	0.17	0.18	0.05	0.05
Benzo(a)pyrene	mg/kg d.b.	< 0.01	< 0.01	< 0.01	< 0.01	< 0.01	0.05	0.11	0.07	0.10	0.06	0.03	0.06
Benzo(b)fluoranthene	mg/kg d.b.	< 0.01	< 0.01	< 0.01	< 0.01	< 0.01	0.06	0.04	0.04	0.06	0.05	0.02	0.11
Benzo(ghi)perylene	mg/kg d.b.	< 0.01	< 0.01	< 0.01	< 0.01	< 0.01	0.04	0.03	0.03	0.04	0.03	0.02	0.08
Benzo(k)fluoranthene	mg/kg d.b.	< 0.01	< 0.01	< 0.01	< 0.01	< 0.01	< 0.01	0.04	0.02	0.02	0.02	0.01	0.11
Chrysene	mg/kg d.b.	< 0.01	< 0.01	< 0.01	< 0.01	< 0.01	0.01	0.36	0.24	0.34	0.27	0.07	0.08
Dibenzo(a.h)anthracene	mg/kg d.b.	< 0.01	< 0.01	< 0.01	< 0.01	< 0.01	0.02	0.03	0.02	0.03	0.02	0.01	0.07
Phenanthrene	mg/kg d.b.	0.04	< 0.01	0.06	< 0.01	< 0.01	2.62	4.20	3.62	1.25	2.51	1.22	< 0.01
Fluoranthene	mg/kg d.b.	< 0.01	< 0.01	< 0.01	< 0.01	< 0.01	0.52	0.54	0.50	0.40	0.71	0.21	< 0.01
Fluorene	mg/kg d.b.	< 0.01	< 0.01	< 0.01	< 0.01	< 0.01	1.44	1.95	2.31	0.46	1.52	0.79	< 0.01
Indeno(1.2.3-cd)pyrene	mg/kg d.b.	< 0.01	< 0.01	< 0.01	< 0.01	< 0.01	0.03	0.01	0.01	0.02	0.01	< 0.01	0.07
Naphthalene	mg/kg d.b.	0.11	0.22	0.19	0.10	< 0.01	3.97	0.02	< 0.01	0.13	0.03	0.01	0.51
Pyrene	mg/kg d.b.	< 0.01	< 0.01	< 0.01	< 0.01	< 0.01	0.55	0.71	0.59	0.47	0.54	0.26	< 0.01
Total EPA-PAH (by calculation)	mg/kg d.b.	0.14	< 0.01	0.26	0.10	< 0.01	13.18	9.55	9.09	4.08	6.98	3.30	1.17
Total EFSA-PAH (by calculation)	mg/kg d.b.	<0.01	<0.01	<0.01	<0.01	<0.01	0.3	0.9	0.6	0.8	0.6	0.2	0.6

The biochars were analysed at Water & Life lab according to methods for PAH CEN/TS 16181: 2018. Results are presented in Table 25. Regarding the PAH-Content the EBC states that for agricultural application the total sum of the 16 EPA-PAH must not be above 6±2.4 mg/kg $_{d.b.}$ and the total sum of the 8 EFSA-PAH must not be above 1.0 mg/kg $_{d.b.}$(EBC, 2022). Looking at Table 25 it is clearly visible that the second condition from the EBC is fulfilled for every biochar sample. The first condition on the total sum of 16 EPA-PAH is fulfilled for all samples except 1.BC.PL, 3-BC.PL and 7.BC.GP. These samples would not be suitable for agricultural applications regarding their PAH content. In general, the average total sum of 16 EPA-PAH for the pyrolysis samples was 5.7±3.1 and for the gasification samples 3.42±5.6 mg/kg $_{d.b.}$. This is probably in large part due to the differences in technologies used (take gasification for example, there the pilot-biochar contains way more PAH than the lab-scale-chars), as the type of reactor and the process conditions have great impact on PAH-content in biochars (although feedstock related effects can also play a role) (Buss *et al.,* 2016).

4.1.5 PCB & PCDD/PCDF Measurements

Water & Life lab performed the Polychlorinated biphenyls (PCB) analyses according to EPA 3550 C 2007 + EPA 8270 E 2018. The results are presented in Table 26. There was no detectable PCB concentration in either of the pilot chars to be found.

Table 26: PCB results of the biochar gasification pilotscale sample made of wood affected by bark beetles - 7.BC.GP and the biochar pilotscale pyrolysis samples made from walnut shells - 3.BC.PP WS; BC stands for biochar; PP stands for pyrolysis pilotscale; GP stands for gasification pilotscale;

		7.BC.GP	3.BC.PP
PCB	unit		
PCB 28 (TriCB)	mg/kg	< 0.01	< 0.01
PCB 52 (TetraCB)	mg/kg	< 0.01	< 0.01
PCB 77 (TetraCB)	mg/kg	< 0.01	< 0.01
PCB 81 (TetraCB)	mg/kg	< 0.01	< 0.01
PCB 91 (TetraCB)	mg/kg	< 0.01	< 0.01
PCB 99 (PentaCB)	mg/kg	< 0.01	< 0.01
PCB 101 (PentaCB)	mg/kg	< 0.01	< 0.01
PCB 105 (PentaCB)	mg/kg	< 0.01	< 0.01
PCB 110 (PentaCB)	mg/kg	< 0.01	< 0.01
PCB 114 (PentaCB)	mg/kg	< 0.01	< 0.01
PCB 128+123 (PentaCB)	mg/kg	< 0.01	< 0.01
PCB 126 (PentaCB)	mg/kg	< 0.01	< 0.01
PCB 128 (HexaCB)	mg/kg	< 0.01	< 0.01
PCB 138 (HexaCB)	mg/kg	< 0.01	< 0.01
PCB 146 (HexaCB)	mg/kg	< 0.01	< 0.01
PCB 149 (HexaCB)	mg/kg	< 0.01	< 0.01
PCB 151 (HexaCB)	mg/kg	< 0.01	< 0.01
PCB 153 (HexaCB)	mg/kg	< 0.01	< 0.01
PCB 156 (HexaCB)	mg/kg	< 0.01	< 0.01

PCB 157 (HexaCB)	mg/kg	< 0.01	< 0.01
PCB 167 (HexaCB)	mg/kg	< 0.01	< 0.01
PCB 169 (HexaCB)	mg/kg	< 0.01	< 0.01
PCB 170 (HeptaCB)	mg/kg	< 0.01	< 0.01
PCB 177 (HeptaCB)	mg/kg	< 0.01	< 0.01
PCB 180 (HeptaCB)	mg/kg	< 0.01	< 0.01
PCB 183 (HeptaCB)	mg/kg	< 0.01	< 0.01
PCB 187 (HeptaCB)	mg/kg	< 0.01	< 0.01
PCB 189 (HeptaCB)	mg/kg	< 0.01	< 0.01
PCB sums (D.Lgs. n. 121 del 03/09/2020) mg/kg < 0.01	mg/kg	< 0.01	< 0.01
PCB sums (Reg. CE 2019/1021 e s.m.i.)	mg/kg	< 0.01	< 0.01

Water & Life lab performed the Dioxin and furan analyses according to EPA 8280 B 2007. The results are presented in Table 27. Except for 2.3.7.8 TCDF in the 7.BC.GP sample, none of the analysed dioxin and furan pollutants were detected. The maximum of detectable PCDD/PCDFs is with 0.0059 µg/kg way below the EBC threshold of 0.02 µg/kg. for the EBC-Agro certificates (EBC, 2022). For the EBC-Feed category a threshold of <0.0005 is needed, thus requiring more sensitive analytics.

Table 27: Dioxins and furans results of the biochar gasification pilotscale sample made of wood affected by bark beetles - 7.BC.GP and the biochar pilotscale pyrolysis samples made from walnut shells - 3.BC.PP WS; BC stands for biochar; PP stands for pyrolysis pilotscale; GP stands for gasification pilotscale;

DIOXINS AND FURANS		**7.BC.GP**	**3.BC.PP**
PCDD:	unit		
2.3.7.8 TCDD	µg/kg	< 0.0010	< 0.0010
1.2.3.7.8 PCDD	µg/kg	< 0.0050	< 0.0050
1.2.3.4.7.8 HxCDD	µg/kg	< 0.0050	< 0.0050
1.2.3.7.8.9 HxCDD	µg/kg	< 0.0050	< 0.0050
1.2.3.6.7.8 HxCDD	µg/kg	< 0.0050	< 0.0050
1.2.3.4.6.7.8 HpCDD	µg/kg	< 0.0050	< 0.0050
OCDD	µg/kg	< 0.0100	< 0.0100
PCDF:			
2.3.7.8 TCDF	µg/kg	0.0021	< 0.0010
2.3.4.7.8 PCDF	µg/kg	< 0.0050	< 0.0050
1.2.3.7.8 PCDF	µg/kg	< 0.0050	< 0.0050
1.2.3.4.7.8 HxCDF	µg/kg	< 0.0050	< 0.0050
1.2.3.7.8.9 HxCDF	µg/kg	< 0.0050	< 0.0050
1.2.3.6.7.8 HxCDF	µg/kg	< 0.0050	< 0.0050
2.3.4.6.7.8 HxCDF	µg/kg	< 0.0050	< 0.0050
1.2.3.4.6.7.8 HpCDF	µg/kg	< 0.0050	< 0.0050
1.2.3.4.7.8.9 HpCDF	µg/kg	< 0.0050	< 0.0050
OCDF	µg/kg	< 0.0100	< 0.0100
Sum of PCDD/PCDF	µg/kg	0.0059	0.0057

4.1.6 X-ray Powder Diffraction (XRD)

The samples were analyzed using powder X-ray diffraction (XRD) using the PANalytical X'Pert Pro instrument. The CuKα1 radiation source was used for the scanning from 10° to 80°.
The graphical representations of the results are presented below. The diffractograms are displayed in two modes for samples from unibz and BEST. The results from the XRD analysis are shown in Figure 18 to Figure 22 and Figure 24.

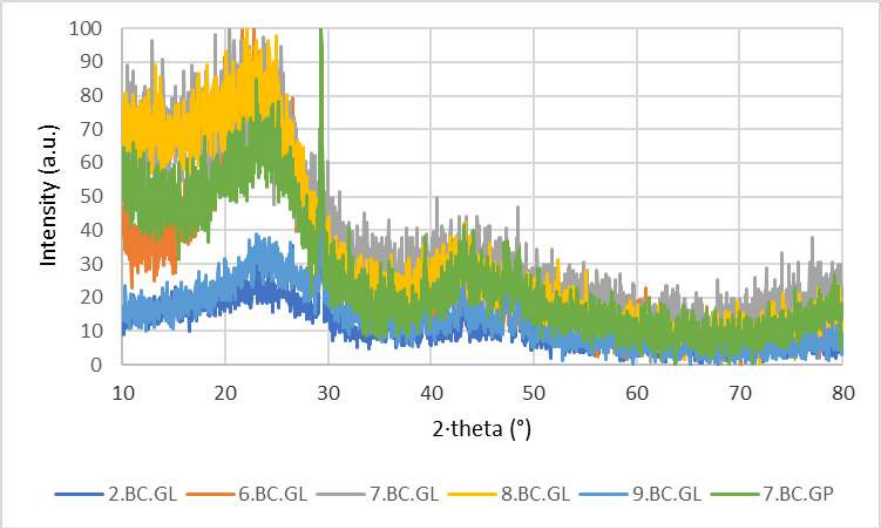

Figure 18: xrd1. Absolute comparison of XRD spectra of the biochar gasification samples made from river woody debris - 2.BC.GL; spelt husks - 6.BC.GL; wood affected by bark beetles - 7.BC.GL; chestnut wood without tannins - 8.BC.GL; vine prunings - 9.BC.GL; wood affected by bark beetles - 7.BC.GP;

Two broad signals at 23° and 44° were observed relating to turbostratic carbon.

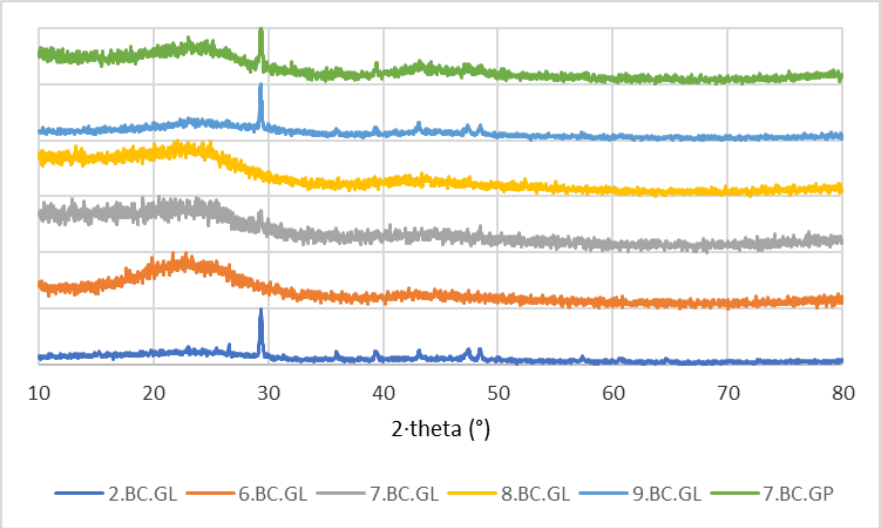

Figure 19: xrd2. Relative comparison of XRD stacked spectra of the biochar gasification samples made from river woody debris - 2.BC.GL; spelt husks - 6.BC.GL; wood affected by bark beetles - 7.BC.GL; chestnut wood without tannins - 8.BC.GL; vine prunings - 9.BC.GL; wood affected by bark beetles - 7.BC.GP;

In addition to the peak relating to the turbostratic carbon, we can observe several small peaks at 29.4° which probably relates to some inorganic impurities, although we cannot observe this signal from the same source (wood affected by bark beetles) and different treatments (7.BC.GP and 7.BC.GL). The presence of ordered graphite is excluded since graphite (002) reflection appears between 26° and 28° of 2 θ (Khan *et al.*, 2019).

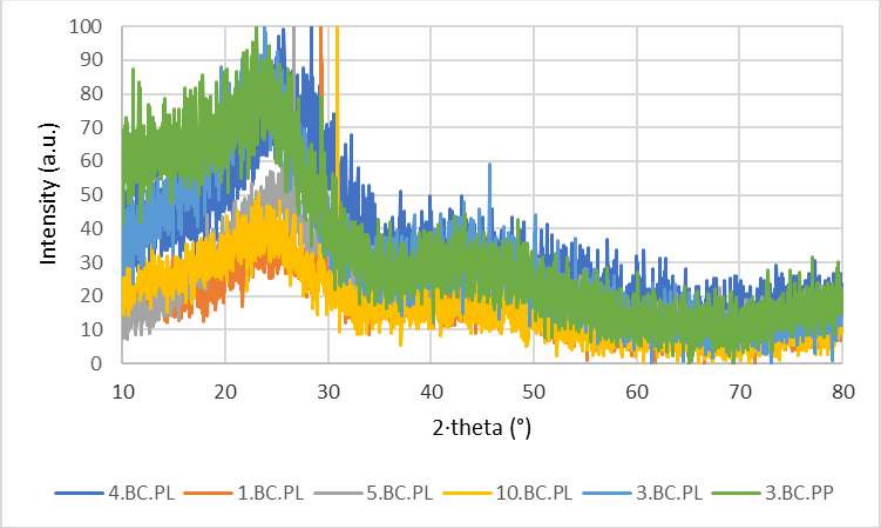

Figure 20: xrd3. Absolute comparison of XRD spectra of the biochar pyrolysis samples made from coffee husks - 1.BC.PL; walnut shells - 3.BC.PL; bran 4.BC.PL; Compost screenings - 5.BC.PL; wood chips from broadleaf forestry sites - 10.BC.PL; walnut shells - 3.BC.PP WS;.

Similar than with the unibz samples we can clearly observe two broad signals at 23° and 44° relating to turbostratic carbon.

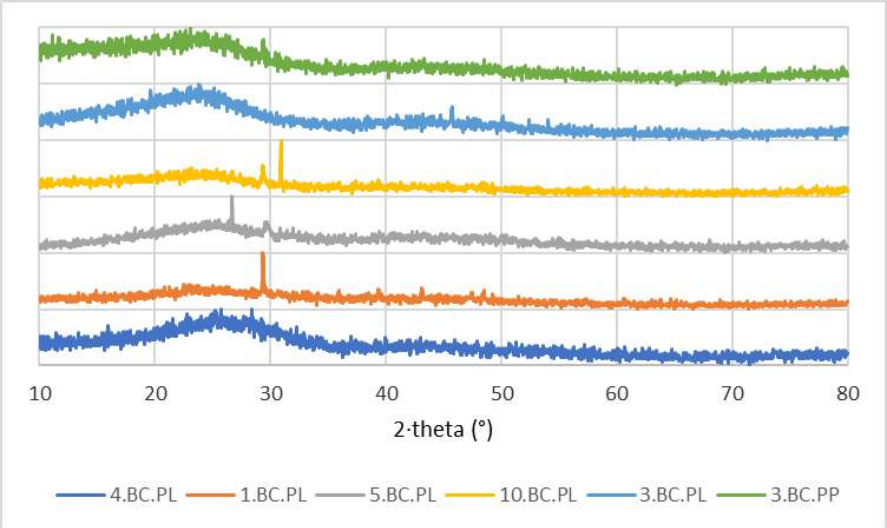

Figure 21: xrd 4. Relative comparison of XRD stacked spectra of the biochar pyrolysis samples made from coffee husks - 1.BC.PL; walnut shells - 3.BC.PL; bran 4.BC.PL; Compost screenings - 5.BC.PL; wood chips from broadleaf forestry sites - 10.BC.PL; walnut shells - 3.BC.PP WS;.

Again, in addition to the peak relating to the turbostratic carbon, several small peaks at 29.4° (sample 10.BC.PL and 1.BC.PL) and at 30.9° (sample 10.BC.PL) were observed which probably

relates to some inorganic impurities. When comparing the signal from the same source (walnut shells) and different treatments (3.BC.PP and 3.BC.PL) we can observe that the diffractograms are very similar, with no distinct difference showing high consistency during scale up. Again, the mayor presence of ordered graphite is excluded since graphite (002) reflection appears between 26° and 28° of 2 θ (Khan *et al.*, 2019).

The diffractograms did not show large narrow crystalline peaks, which is typical for biochar samples treated at low temperature (< 2000 °C). At higher temperatures a graphite structure is produced with (main) (002) reflection at 26°-28° (Khan *et al.*, 2019). Although the temperature of graphitization could be lowered using inexpensive iron- or magnesium-based catalyst to 1200 °C (Lower *et al.*, 2023). XRD diffractogram of the graphite standard can be found in Figure 22. We did not observe consistent presence of such signal in the biochar samples. However, we observed the consistent signals at 23° and at 44° relating to turbostratic carbon.

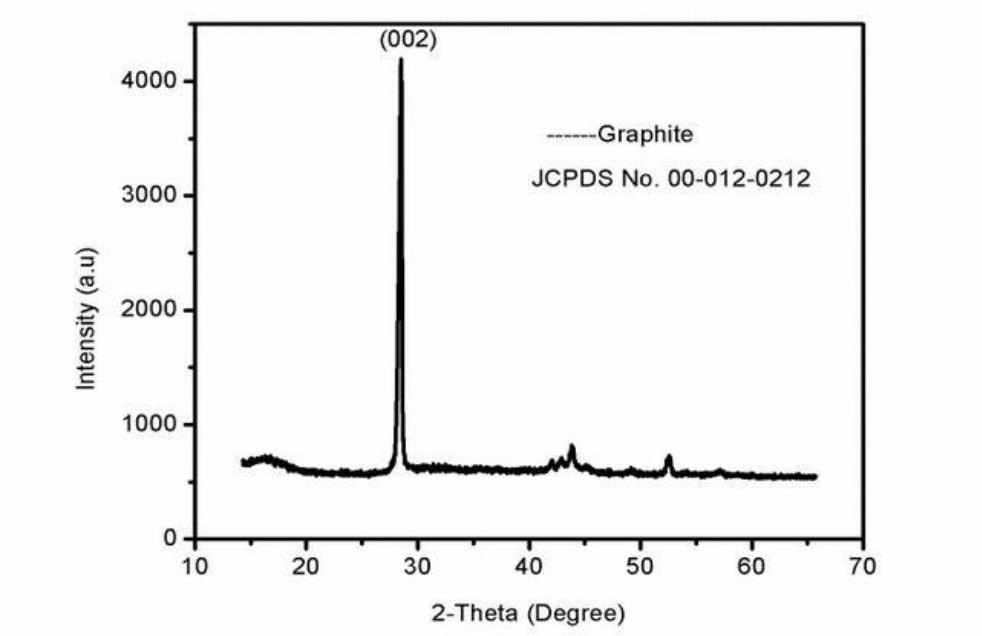

Figure 22: The graphite(002) reflection can be observed between 26° and 28° (Khan et al.*, 2019).*

In the course of calcining, carbon gradually combines to create a substance characterized by a turbostratic structure, as depicted in Figure xrd6. In the subsequent process of graphitization, the turbostratic carbon undergoes increased organization, ultimately culminating in the formation of highly ordered, crystalline graphite (Lower *et al.*, 2023). The decline in CEC (cation exchange capacity) results from the elimination of surface functional groups and the development of more organized structure. Multiple investigations have noted that the cation exchange capacity of biochar diminishes as the pyrolysis temperature increases (Tomczyk *et al.*, 2020). Therefore, the balance between long term carbon sequestration stability and certain functional parameters such nutrient capacity or other requirements for specific application needs to be reached.

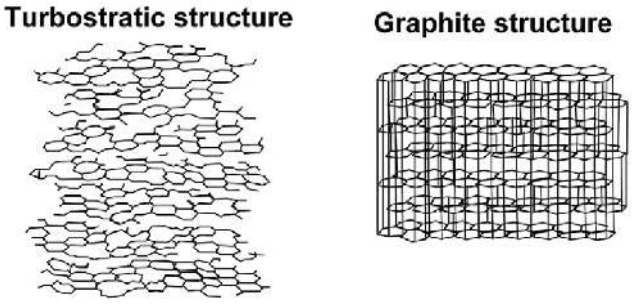

Figure 23: The illustration of turbostratic and graphitic carbon

For comparison when increasing the pyrolysis temperature from 300 °C to 600 °C the cellulose breaks down to form turbostratic carbon, as evidenced from decrease of (101) peaks relating to cellulose. We can see that with temperature increase the (002) peaks narrow, meaning that the structure is becoming more ordered (Pusceddu *et al.*, 2017).

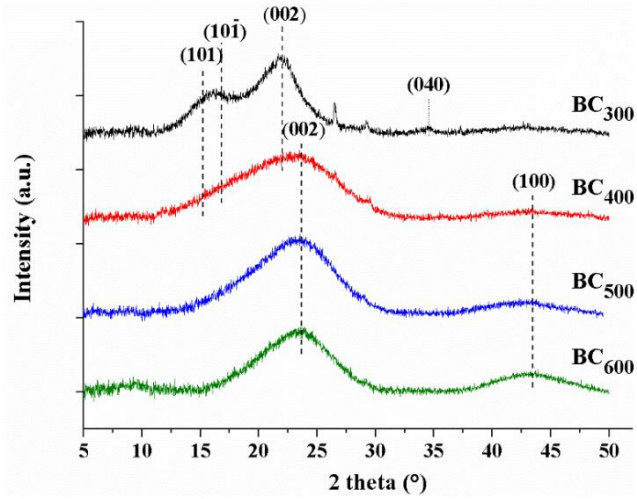

Figure 24: The XRD spectres of biochar samples prepared at different pyrolysis temperatures (300 °C. 400 °C. 500 °C and 600 °C) (Pusceddu et al., 2017).

A similar ratio of (002)-23° to (100)-44° peak height in the present case was observed. For quantitative determination of crystallinity index, additional experiments would have to be performed to obtain reliable values. Overall, we can confirm, based on diffractograms, consistency with literature data and very high consistency between laboratory and pilot scale experiments

4.1.7 Thermogravimetry (TG)

The thermogravimetric measurements were performed using the PerkinElmer EGA 4000 instrument and had three steps:

1. holding the sample at 40 °C for 1 minute.
2. heating from 40 °C to 700 °C with heating rate of 10 K/min and nitrogen gas (N_2) volumetric flow rate of 50 ml/min and
3. holding the sample at 700 °C for 30 minutes.

The results of the second TG step are presented in the figures below (Figure 25 to Figure 28).

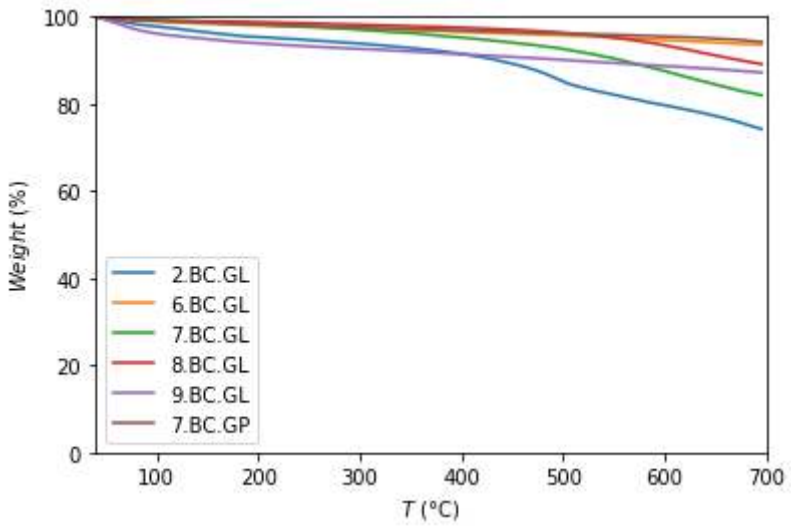

Figure 25: Weight of the biochar gasification samples made from river woody debris - 2.BC.GL; spelt husks - 6.BC.GL; wood affected by bark beetles - 7.BC.GL; chestnut wood without tannins - 8.BC.GL; vine prunings - 9.BC.GL; wood affected by bark beetles - 7.BC.GP - during TG measurements.

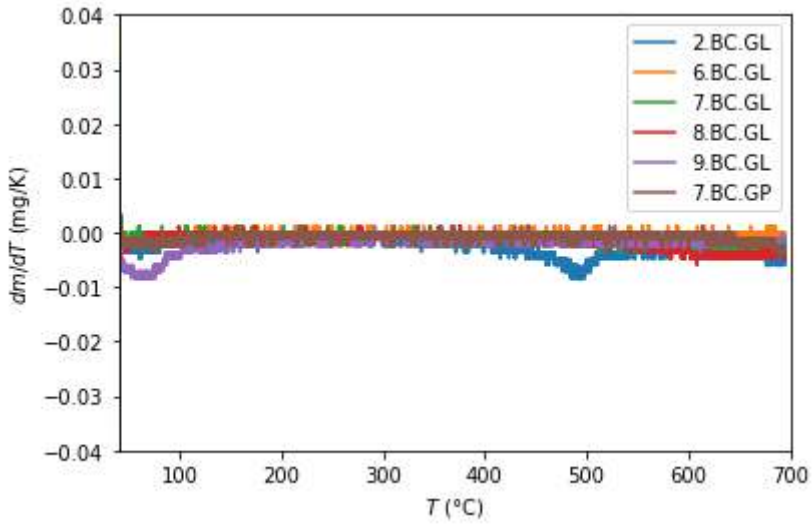

Figure 26: Weight loss of the biochar gasification samples made from river woody debris - 2.BC.GL; spelt husks - 6.BC.GL; wood affected by bark beetles - 7.BC.GL; chestnut wood without tannins - 8.BC.GL; vine prunings - 9.BC.GL; wood affected by bark beetles - 7.BC.GP - during TG measurements.

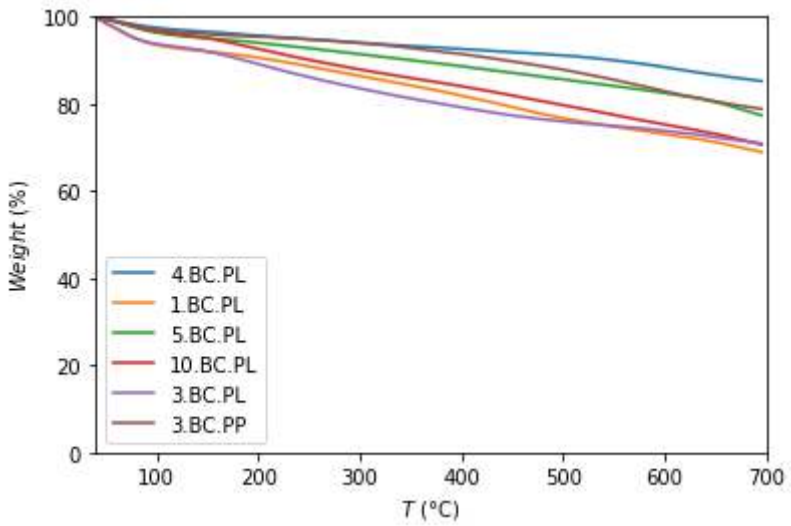

Figure 27: Weight of the biochar pyrolysis samples made from coffee husks - 1.BC.PL; walnut shells - 3.BC.PL; bran 4.BC.PL; Compost screenings - 5.BC.PL; wood chips from broadleaf forestry sites - 10.BC.PL; walnut shells - 3.BC.PP WS. during TG measurements.

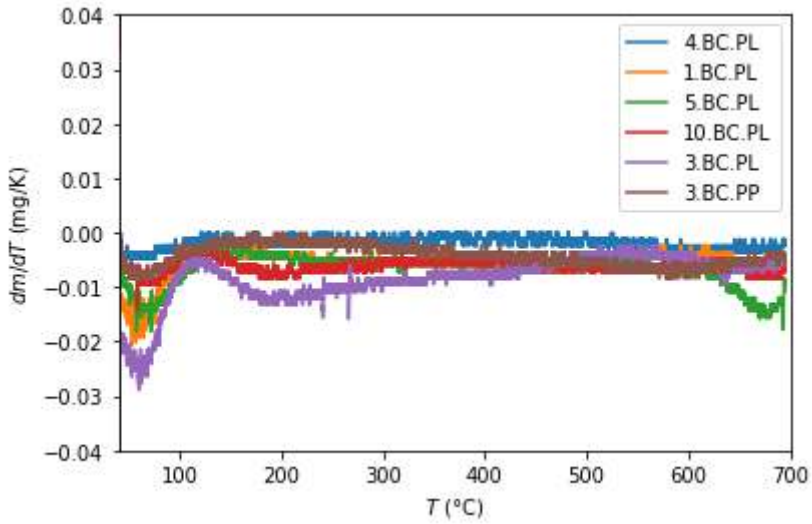

Figure 28: Weight loss of the biochar pyrolysis samples made from coffee husks - 1.BC.PL; walnut shells - 3.BC.PL; bran 4.BC.PL; Compost screenings - 5.BC.PL; wood chips from broadleaf forestry sites - 10.BC.PL; walnut shells - 3.BC.PP WS. during TG measurements.

The TG results show that gasification produces more thermally stable biochar compared to pyrolysis. Of course, the thermal stability of the biochar also varies with different input biomass materials.

4.1.8 pH Measurements

The pH measurements for the Alps4GreenC-project were conducted with a *Metrohm 781 pH/Ion Meter.* The method used was based on the method suggested in the *European Biochar Certificate (EBC)* guidelines (EBC, 2022), meaning that 5 mL biochar sample was suspended in 25 mL 0.01 M $CaCl_2$ solution and shaken for one hour (200 rpm) (EBC, 2022), . Afterwards the pH was measured by inserting the electrode directly into the sample suspension. The pH value

was taken either after a steady pH was reached or after 15 minutes. Before the testing was conducted, some preliminary tests were done. Comparing the method of choice with another method from the literature, using deionized water (Singh *et al.*, 2010). Although the EBC method yielded slightly lower pH-values. the values in total did only differ to a small extent (<0.5 pH units). Table 28 shows the results of the measurements.

Table 28: pH Values for the Alps4GreenC samples

Code	Residue	Production process	pH	T °C
2.BC.GL	river woody debris	gasfication - lab	7.796	22.6
6.BC.GL	spelt husks	gasification - lab	9.258	24
7.BC.GL	wood affected by bark beetles	gasification - lab	7.601	23.1
8.BC.GL	chestnut wood without tannins	gasification - lab	6.941	24.6
9.BC.GL	vine prunings	gasification - lab	8.789	24.5
7.BC.GP	wood affected by bark beetles	gasification - pilot	8.599	25.1
4.BC.PL	bran	pyrolysis - lab	6.723	23.7
1.BC.PL	coffee husks	pyrolysis - lab	9.692	24.2
5.BC.PL	compost screenings	pyrolysis - lab	9.408	23.9
10.BC.PL	wood chips from broadleaf forestry sites	pyrolysis - lab	6.865	24.5
3.BC.PL	walnut shells	pyrolysis - lab	6.149	25.1
3.BC.PP	walnut shells	pyrolysis - pilot	8.319	24.7

The pH-values of the analyzed biochars ranged from slightly acidic to moderately basic, with the lowest determined pH being 6.149 for the lab-scale walnut shells (3.BC.PL) and the highest being 9.692 for the coffee husks (1.BC.PL). Generally speaking, the pH of the biochars was in the expected range, with literature reporting biochar pH values in the range of 6.0 and 11.5 or in some cases even lower or higher (Singh *et al.*, 2017). Three out of four pH values <7 were measured for biochars produced by pyrolysis, with the average pH being 8.164 for gasification and 7.859 for pyrolysis. This is in contrast to the average biochar ash content of 11.1 for gasification and 15.6 for pyrolysis, as a higher ash content usually gives a higher pH (Steiner *et al.*, 2016). This contrast reflects the condensation issue during pyrolysis, as the condensable pyrolysis fraction often contains organic acids like acetic acid (Oasmaa *et al.*, 2009). The condensation issue visible through the difference in pH between the lab and pilot scale biochars. While for the gasification samples the pH difference is 0.998, the pH difference between pyrolysis lab- and pilot-scale is with 2.17 more than twice as high. However, technology or feedstock specific differences cannot be ruled out completely as an explanation for this observation, since both technology and feedstock related influences are unknown.

4.1.9 Scanning Electron Microscopy (SEM)

Scanning electron microscopy was carried out with the HR-SEM Zeiss Supra 35 VP instrument. The samples observed were the biochars produced from wood affected by bark beetles (gasification) and walnut shells (pyrolysis) in labscale and pilotscale experiments 7.BC.GL &

7.BC.GP (wood affected by bark beetles) and 3.BC.PL & 3.BC. PP (walnut shells). The pictures of the SEM analysis are shown in Figure 29 to Figure 32.

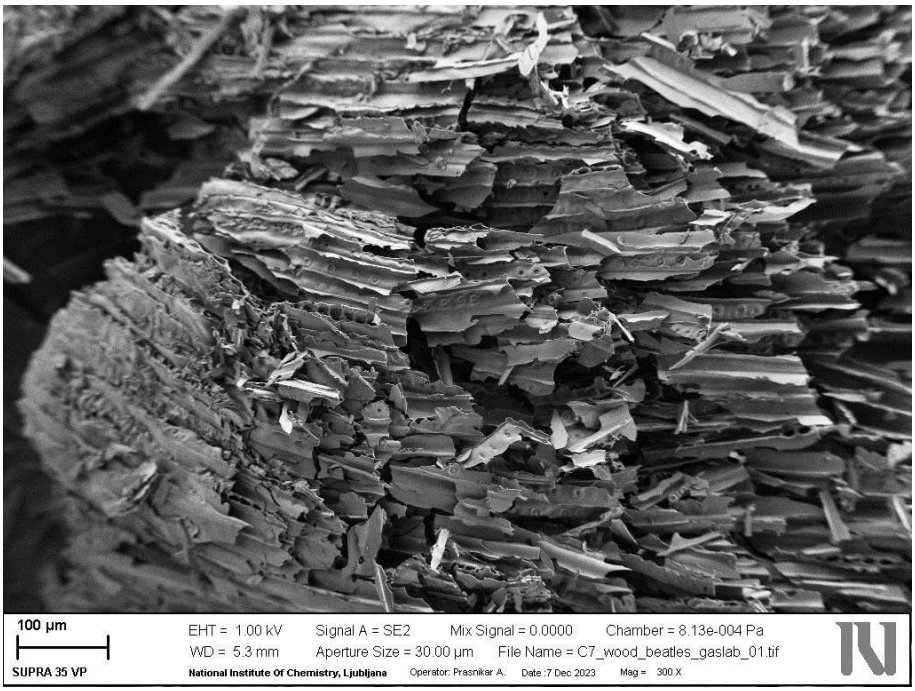

Figure 29: SEM image of the biochar labscale gasification sample wood affected by bark beetles 7.BC.GL.

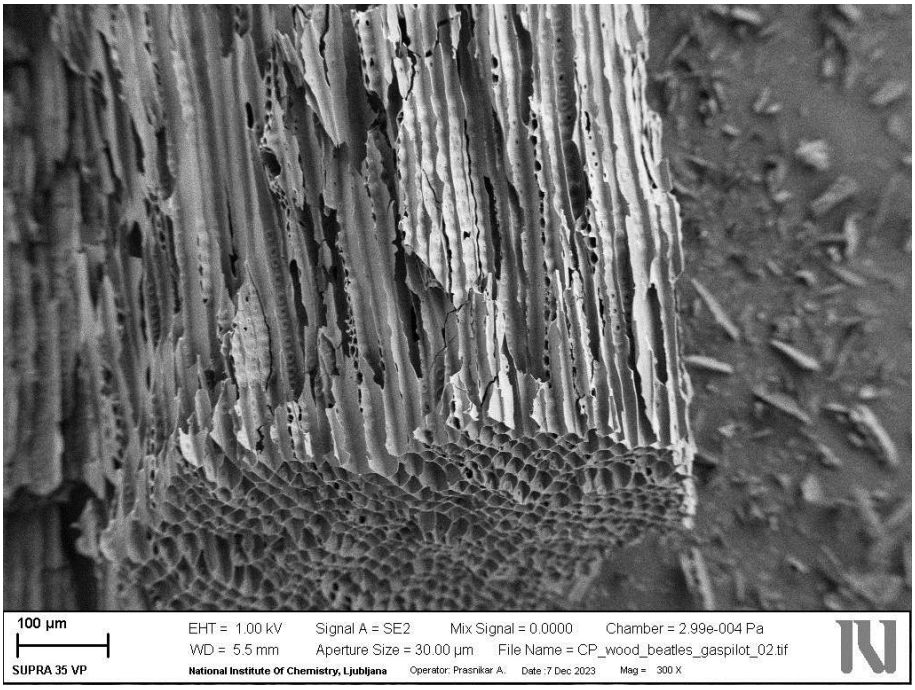

Figure 30: SEM image of biochar pilotscale gasification sample wood affected by bark beetles 7.BC.GP.

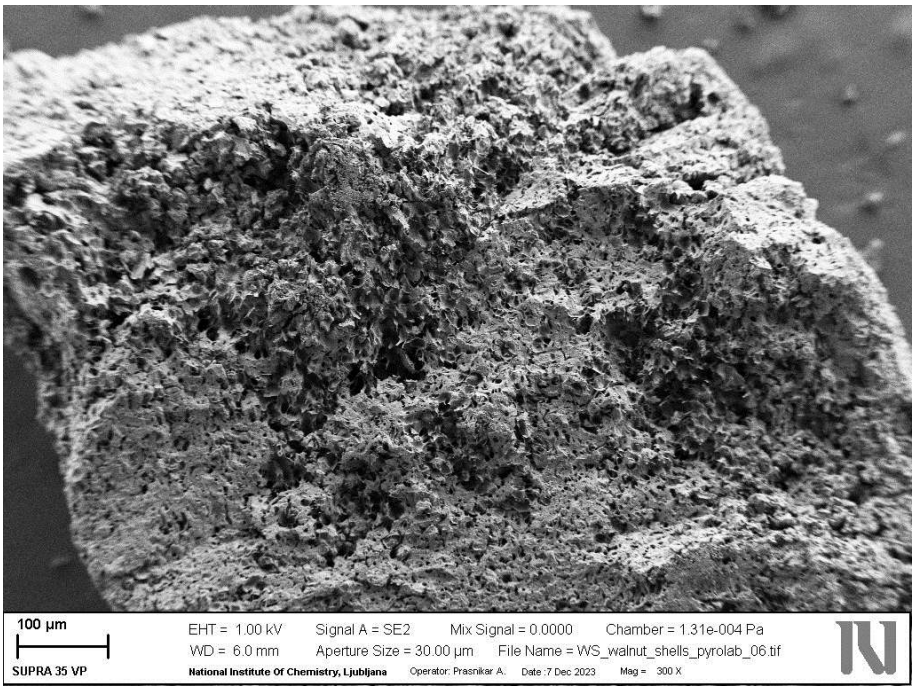

Figure 31: SEM image of the biochar labscale pyrolysis sample walnut shells 3.BC.PL.

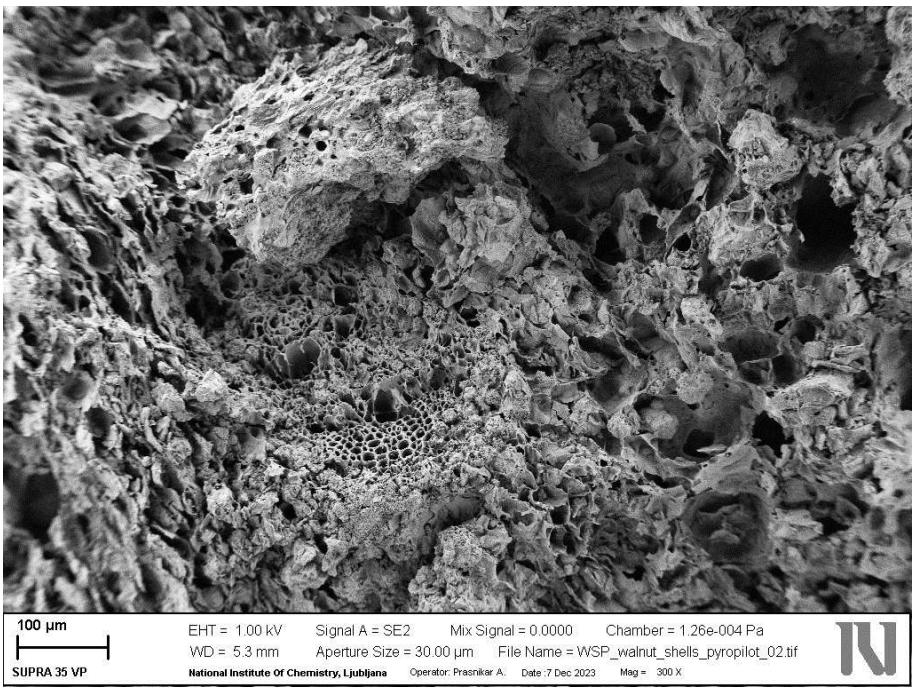

Figure 32: SEM image of the biochar pilotscale pyrolysis sample walnut shells 3.BC.PP.

The surface structures observed with SEM seem to be similar between the laboratory and the pilot scale biochar production methods while observing biochars from the same input biomass materials. Therefore, the surface properties seem to be mostly affected by the input material.

4.1.10 ATR-FTIR spectroscopy

The biochar ATR FTIR characterizations were made with the PerkinElmer Spectrum Two instrument, which measured in the mid-IR spectrum (4000 - 400 cm^{-1}) with 16 scans and resolution of 4 cm^{-1}. The graphical representations of the results are presented below (Figure 33 to Figure 36).

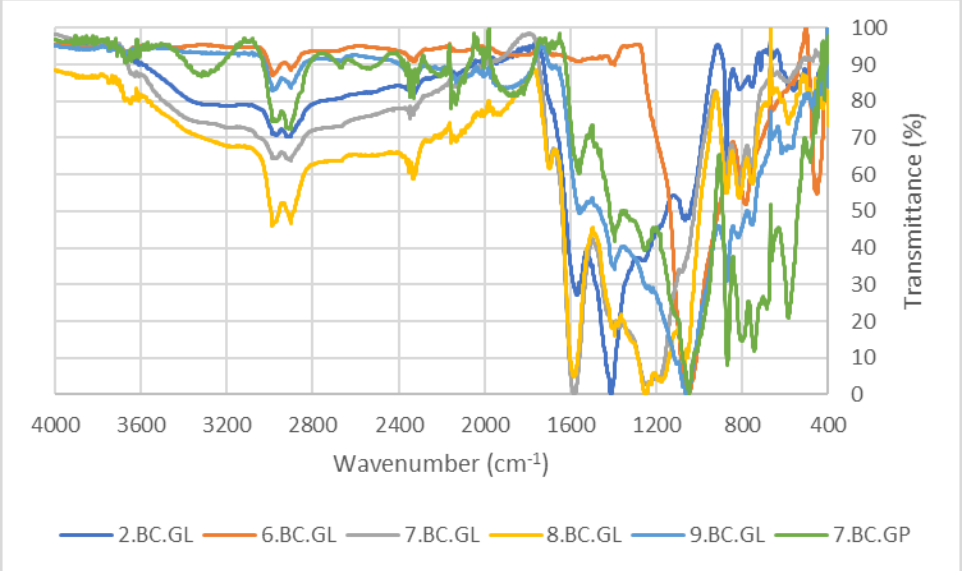

Figure 33: ATR-FTIR spectra of the biochar gasification samples made from river woody debris - 2.BC.GL; spelt husks - 6.BC.GL; wood affected by bark beetles - 7.BC.GL; chestnut wood without tannins - 8.BC.GL; vine prunings - 9.BC.GL; wood affected by bark beetles - 7.BC.GP.

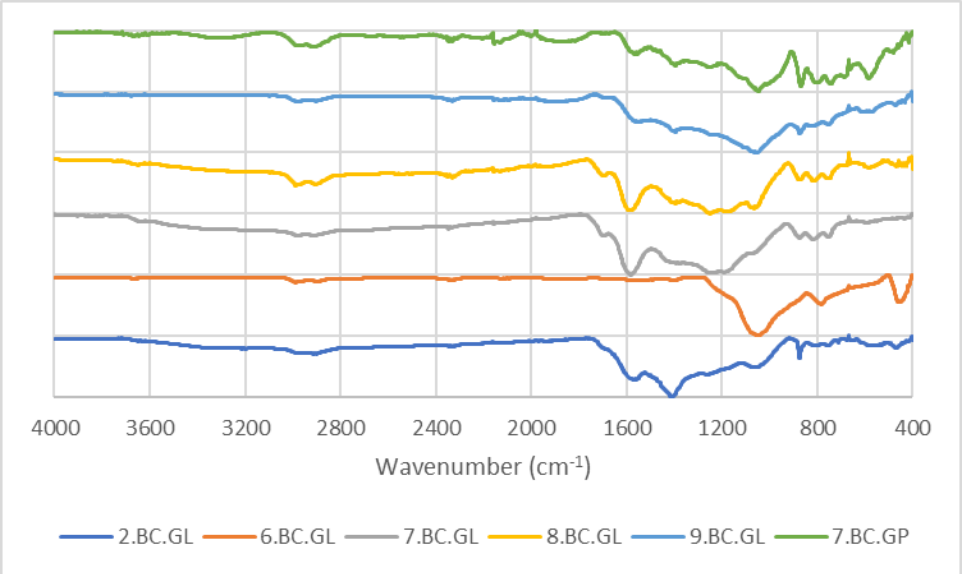

Figure 34: ATR-FTIR stacked spectra of the biochar gasification samples made from river woody debris - 2.BC.GL; spelt husks - 6.BC.GL; wood affected by bark beetles - 7.BC.GL; chestnut wood without tannins - 8.BC.GL; vine prunings - 9.BC.GL; wood affected by bark beetles - 7.BC.GP.

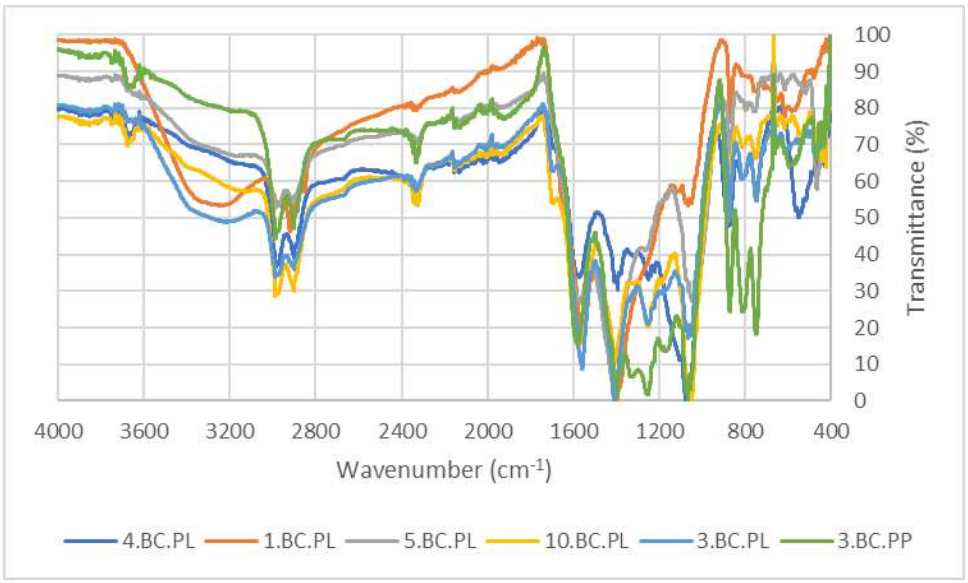

Figure 35: ATR-FTIR spectra of the biochar pyrolysis samples made from coffee husks - 1.BC.PL; walnut shells - 3.BC.PL; bran 4.BC.PL; Compost screenings - 5.BC.PL; wood chips from broadleaf forestry sites - 10.BC.PL; walnut shells - 3.BC.PP WS.

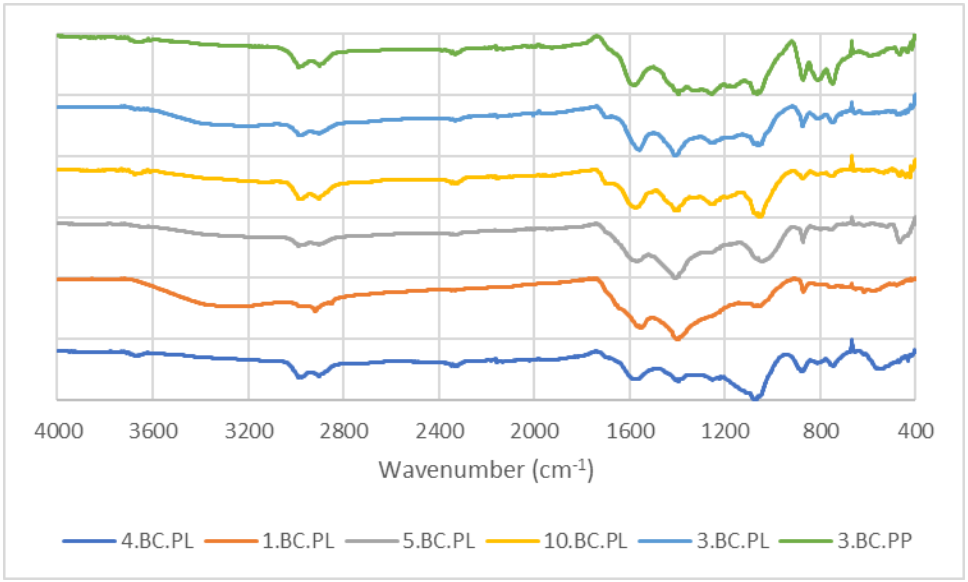

Figure 36: ATR-FTIR stacked spectra of the biochar pyrolysis samples made from coffee husks - 1.BC.PL; walnut shells - 3.BC.PL; bran 4.BC.PL; Compost screenings - 5.BC.PL; wood chips from broadleaf forestry sites - 10.BC.PL; walnut shells - 3.BC.PP WS.

List of the possible functional groups observed at the biochar samples:

- O-H stretching - carboxylic acid. 3500 - 2500 cm^{-1}. broad. intense
- O-H stretching - alcohol. 3300 cm^{-1}. broad. medium
- C-H stretching - aliphatic. 3000 - 2900 cm^{-1}. sharp. medium
- C=O stretching - unsaturated carboxylic acid. ~ 1700 cm^{-1}. sharp. medium
- C=C stretching - unsaturated. 1583 cm^{-1}. sharp. intense
- O-H bending. 1410 cm^{-1}. sharp. intense
- C-O stretching - primary alcohol. 1048 cm^{-1}. sharp. intense

- C-H bending - trisubstituted aromatic. 900 - 700 cm^{-1}. intense
- C-H bending - disubstituted aromatic. ~ 800 cm^{-1}. intense
- C-H bending - monosubstituted aromatic. ~ 750 cm^{-1}. intense

The functional groups were identified with basic knowledge of the biochar materials and use of the IR Spectrum Table & Chart. available at: https://www.sigmaaldrich.com/SI/en/technical-documents/technical-article/analytical-chemistry/photometry-and-reflectometry/ir-spectrum-table

The ATR FTIR results show significant difference between the sample 6.BC.GL and all of the other gasified samples; The differences mainly occur in the region of wavenumbers from 1800 to 1000 cm^{-1} (C=O stretching. C=C stretching. O-H bending and C-O stretching). The reason for this could be the fact that 6.BC.GL is not a wood-based material, while most of the other gasified materials except 9.BC.GL are wood-based materials. The 9.BC.GL sample has a much smaller peak at 1583 cm^{-1} (C=C stretching), compared to the wood-based materials. If we compare the 7.BC.GL and 7.BC.GP samples, they have similar FTIR spectra, but are not identical e.g. 7.BC.GL has a more pronounced peak at 1583 cm^{-1} (C=C stretching). The pyrolyzed samples all produce similar FTIR spectra with the exception of sample 4.BC.PL. which has a less intense peak at 1048 cm^{-1} (C-O stretching). The FTIR spectra of the 3.BC.PL and 3.BC.PP samples are almost identical, which means that pyrolysis on laboratory and pilot scale produces similar biochar (from the same biomass residue). One relevant peak where the 3.BC.PL and 3.BC.PP samples differ is the broad band from about 2500-3500 cm^{-1} present in the 3.BC.PL and missing in the 3.BC.PP sample. Since this band usually relates to alcohol or carboxylic acids functionalities, it would again reflect the condensation issue with the rotary kiln, as condensable pyrolysis liquids often contain alcohols and organic acids (Oasmaa *et al.*, 2012). The same band is clearly visible for the 1.BC.PL sample and debatable for the 5.BC.PL and 10.BC.PL samples.

5 Summary and Conclusion

In the course of the activity 1.3 Practical testing and pilot production of green carbon the Deliverable 1.3.1 Alps4GreenC Testing and pilot production report is created.
This report presents the methodology used for 10 biomass residues analyses. That 10 residues are selected for laboratory tests, 5 for gasification tests at unibz and 5 for pyrolysis tests at BEST. Afterwards, tests at pilot scale are conducted for pyrolysis of 1 residue at BEST and for gasification of 1 residue at unibz.
The produced biochars in lab and pilot tests are sent to NIC for analyses and evaluation of its suitability for sustainable use in agriculture and steel industry. Further biochar analyses are performed from the external laboratory Water & Life Lab (Italy) and the project partner unibz. The produced biochars were analyzed for elemental analyses (C, H, N, S), moisture and ash content. Moreover, the higher heating value was calculated according to the Milne's formula. The biochars were characterized with X-ray Powder Diffraction (XRD), Thermogravimetry (TG), pH measurements, Scanning Electron Microscopy (SEM) and ATR-FTIR spectroscopy.

5.1 Application in Steel and Agriculture

As the application in steel industry often requires a low (<10-15 w/w%) ash content (Quicker and Weber, 2016) the application of the ash-rich chars produced for the residues of bran, compost screenings, spelt husks, coffee husks and vine prunings could face some issues in this field. However, there might be some processes that are more resistant to higher ash contents. And one could even try to remove some of the ash could be removed to improve the fuel quality, as demonstrated in Mukhopadhyay *et al.* in 2022. On the other hand, the biochars low in ash content also show high heating values and low S contents, which both are desirable properties in steel industry. All in all, it can be said that some of the produced chars might face considerable issues for their application in steel industry due to their high ash and low energy content. While other biochars, mainly produced from woody biomass, do show more advantageous properties in that regard.

The application of biochar in agriculture either as a soil amendment or a feed additive is a promising option for all of the produced biochars. Whether it is due to the low pollutant concentration or due to the high content of nutrient elements – None of the chars are excluded in principle from agricultural application. Some, however, would face some issues with their heavy metal content, which could be overcome with a little bit of troubleshooting. One could either change the process parameters to get a higher yield in solids and thus a lower concentration in heavy metals or add some residue with little heavy metals before the process to dilute the resulting biochar. In the case of the coffee husks, one reason for the elevated concentrations could also be due to seasonal variations or differences in varieties of coffee. For future experiments in the lab scale pyrolysis and pilot scale gasification a change in process conditions and/or reactor setup is definitely necessary to reduce PAH content in the produced biochars.

5.2 Outlook

The crowdsourcing campaign in the project showed that a large number and wide range of biomass residues are suitable for valorization in biochar by using pyrolysis or gasification. Moreover, the project results indicated that various biomass residue and their produced biochar for different applications.

The use of biochar in agriculture and the steel industry extends beyond the duration of this project and is being considered for in a further project proposal of **AlpBioCarbon** - Sustainable Green Carbon Production for Circular Bioeconomy in the Alpine region. This applied project is an Interreg Alpine Space classic project.

6 Figures and Tables

Figure 1: The 16x16 mm sieve apparatus made by FleXiever located at BEST, used to sieve sample 10 12
Figure 2: Top: The coffee husks in their final form after processing; Bottom: The second batch of coffee husks at BEST, set for pyrolysis 12
Figure 3: The used rotary kiln system, with the residue storage marked in red. 13
Figure 4: A picture of the reactor inside, taken from the exit of the drum. It represents the beginning of the heated reactor zone, where clearly visible the bran biochar accumulated . 15
Figure 5: A detailed drawing of the lab-scale pyrolysis reactor. Marked in red is the hot zone of the reactor, marked in blue are the cool zones and marked in orange is the gas exit. 16
Figure 6: A) Picture of the gas outlet located in the hot reactor core. It can be clearly seen that the exit for the syngas is blocked by biochar particles. B) Exemplary picture of the tar deposition issue, located at the feeding screw 16
Figure 7: left: Pilot Scale pyrolysis plant from outside; right: pyrolysis plant inside container, pyrolysis reactor on left and gas burner on right side 18
Figure 8: Course of temperature and air gas streams during pyrolysis test with walnut shells 19
Figure: 9 Chipping machine (Tritone Maxi by Ceccato Olindo s.r.l.) 20
Figure 10: Test sieve machine (Titan 450 by Endecotts Ltd.) 20
Figure 11: Schematic of lab-scale gasification system 21
Figure 12: Lab-scale gasifier – mounted on weighing scale (L), during operation (R) 21
Figure 13: Mass fraction of biochar (%) as a function of: (a) Size index, (b) Maximum temperature, (c) Moisture content. 23
Figure 14: Interaction effects between residue moisture content (a), particle size (b), and maximum temperatures (c) achieved during gasification. 24
Figure 15: Schematic of pilot scale gasification system 26
Figure 16: Pilot scale gasification setup 26
Figure 17: Locations of the various temperature measurement points along the reactor 28
Figure 18: xrd1. Absolute comparison of XRD spectra of the biochar gasification samples made from river woody debris - 2.BC.GL; spelt husks - 6.BC.GL; wood affected by bark beetles - 7.BC.GL; chestnut wood without tannins - 8.BC.GL; vine prunings - 9.BC.GL; wood affected by bark beetles - 7.BC.GP; 40
Figure 19: xrd2. Relative comparison of XRD stacked spectra of the biochar gasification samples made from river woody debris - 2.BC.GL; spelt husks - 6.BC.GL; wood affected by bark beetles - 7.BC.GL; chestnut wood without tannins - 8.BC.GL; vine prunings - 9.BC.GL; wood affected by bark beetles - 7.BC.GP; 40
Figure 20: xrd3. Absolute comparison of XRD spectra of the biochar pyrolysis samples made from coffee husks - 1.BC.PL; walnut shells - 3.BC.PL; bran 4.BC.PL; Compost screenings - 5.BC.PL; wood chips from broadleaf forestry sites - 10.BC.PL; walnut shells - 3.BC.PP WS; ... 41
Figure 21: xrd 4. Relative comparison of XRD stacked spectra of the biochar pyrolysis samples made from coffee husks - 1.BC.PL; walnut shells - 3.BC.PL; bran 4.BC.PL; Compost screenings - 5.BC.PL; wood chips from broadleaf forestry sites - 10.BC.PL; walnut shells - 3.BC.PP WS; 41

Figure 22: The graphite(002) reflection can be observed between 26° and 28° (Khan et al., 2019)..... 42
Figure 23: The illustration of turbostratic and graphitic carbon..... 43
Figure 24: The XRD spectres of biochar samples prepared at different pyrolysis temperatures (300 °C. 400 °C. 500 °C and 600 °C) (Pusceddu et al., 2017)..... 43
Figure 25: Weight of the biochar gasification samples made from river woody debris - 2.BC.GL; spelt husks - 6.BC.GL; wood affected by bark beetles - 7.BC.GL; chestnut wood without tannins - 8.BC.GL; vine prunings - 9.BC.GL; wood affected by bark beetles - 7.BC.GP - during TG measurements..... 44
Figure 26: Weight loss of the biochar gasification samples made from river woody debris - 2.BC.GL; spelt husks - 6.BC.GL; wood affected by bark beetles - 7.BC.GL; chestnut wood without tannins - 8.BC.GL; vine prunings - 9.BC.GL; wood affected by bark beetles - 7.BC.GP - during TG measurements..... 44
Figure 27: Weight of the biochar pyrolysis samples made from coffee husks - 1.BC.PL; walnut shells - 3.BC.PL; bran 4.BC.PL; Compost screenings - 5.BC.PL; wood chips from broadleaf forestry sites - 10.BC.PL; walnut shells - 3.BC.PP WS. during TG measurements..... 45
Figure 28: Weight loss of the biochar pyrolysis samples made from coffee husks - 1.BC.PL; walnut shells - 3.BC.PL; bran 4.BC.PL; Compost screenings - 5.BC.PL; wood chips from broadleaf forestry sites - 10.BC.PL; walnut shells - 3.BC.PP WS. during TG measurements..... 45
Figure 29: SEM image of the biochar labscale gasification sample wood affected by bark beetles 7.BC.GL..... 47
Figure 30: SEM image of biochar pilotscale gasification sample wood affected by bark beetles 7.BC.GP..... 47
Figure 31: SEM image of the biochar labscale pyrolysis sample walnut shells 3.BC.PL..... 48
Figure 32: SEM image of the biochar pilotscale pyrolysis sample walnut shells 3.BC.PP..... 48
Figure 33: ATR-FTIR spectra of the biochar gasification samples made from river woody debris - 2.BC.GL; spelt husks - 6.BC.GL; wood affected by bark beetles - 7.BC.GL; chestnut wood without tannins - 8.BC.GL; vine prunings - 9.BC.GL; wood affected by bark beetles - 7.BC.GP..... 49
Figure 34: ATR-FTIR stacked spectra of the biochar gasification samples made from river woody debris - 2.BC.GL; spelt husks - 6.BC.GL; wood affected by bark beetles - 7.BC.GL; chestnut wood without tannins - 8.BC.GL; vine prunings - 9.BC.GL; wood affected by bark beetles - 7.BC.GP..... 49
Figure 35: ATR-FTIR spectra of the biochar pyrolysis samples made from coffee husks - 1.BC.PL; walnut shells - 3.BC.PL; bran 4.BC.PL; Compost screenings - 5.BC.PL; wood chips from broadleaf forestry sites - 10.BC.PL; walnut shells - 3.BC.PP WS..... 50
Figure 36: ATR-FTIR stacked spectra of the biochar pyrolysis samples made from coffee husks - 1.BC.PL; walnut shells - 3.BC.PL; bran 4.BC.PL; Compost screenings - 5.BC.PL; wood chips from broadleaf forestry sites - 10.BC.PL; walnut shells - 3.BC.PP WS..... 50

Table 1 Selected residues and their source 4
Table 2: Values gathered from residue analyses compared to data from the Phyllis2 database. All values are based on dry basis (d.b.) and given in % w/w, except for the gross calorific value, which is given in MJ/kg. 6
Table 3: General properties of the analyzed residues 8
Table 4: Calorific values for the different residues 9
Table 5: Nutrient and heavy metal contents of the analyzed residues. All values in mg/kg $_{d.b.}$ * The starred Tests are not ACCREDIA qualified. The used methods: ISO 14780: 2019; ISO 16968:2015 and ISO 6170 :2016 10
Table 6: Particle size distributions for the different samples. All values given in %. Methods used: ISO 14780: 2019; ISO 16968:2015 and ISO 6170: 2016 10
Table 7: Moisture content of the residues selected for pyrolysis, measured before the experiment and during residue analyses 13
Table 8: Process parameters set for each sample during lab-scale pyrolysis 14
Table 9: Results of the lab scale pyrolysis experiments. *including maintenance breaks 17
Table 10: Pretreatment of the used residues 20
Table 11: The moisture content and maximum temperature attained for the various residue and the biochar yield 22
Table 12: Producer gas composition of the experiments conducted on the lab-scale gasifier. 24
Table 13: Mass balances of the experiments conducted on the lab-scale gasifier 25
Table 14: Energy balances of the experiments conducted on the lab-scale gasifier considering 1h of continuous operation. 26
Table 15: Pilot-scale gasification tests on wood affected by bark beetles (BW) 27
Table 16: Average gas composition of the four main tests 27
Table 17**:** Average temperatures recorded at various points along the pilot-scale reactor shown in Figure 17. 28
Table 18: Mass balances of the experiments conducted on the pilot-scale gasifier. 29
Table 19: Energy balances of the experiments conducted on the pilot-scale gasifier considering 1h of continuous operation. 29
Table 20: List of the biochar samples. BC stands for biochar; PL stands for pyrolysis labscale; GL stands for gasification labscale; PP stands for pyrolysis pilotscale; GP stands for gasification pilotscale; 30
Table 21: The results from the analyses done by unibz 31
Table 22: H/C molar and O/C molar ratios for each sample 32
Table 23: Elemental composition of the biochar gasification samples made river woody debris - 2.BC.GL; spelt husks - 6.BC.GL; wood affected by bark beetles - 7.BC.GL; chestnut wood without tannins - 8.BC.GL; vine prunings - 9.BC.GL; wood affected by bark beetles - 7.BC.GP; and the biochar pyrolysis samples made from coffee husks - 1.BC.PL ; walnut shells - 3.BC.PL; bran 4.BC.PL; Compost screenings - 5.BC.PL; wood chips from broadleaf forestry sites - 10.BC.PL; walnut shells - 3.BC.PP WS; BC stands for biochar; PL stands for pyrolysis labscale; GL stands for gasification labscale; PP stands for pyrolysis pilotscale; GP stands for gasification pilotscale; 34

Table 24: Other properties of the biochar gasification samples made river woody debris - 2.BC.GL; spelt husks - 6.BC.GL; wood affected by bark beetles - 7.BC.GL; chestnut wood without tannins - 8.BC.GL; vine prunings - 9.BC.GL; wood affected by bark beetles - 7.BC.GP; and the biochar pyrolysis samples made from coffee husks - 1.BC.PL ; walnut shells - 3.BC.PL; bran 4.BC.PL; Compost screenings - 5.BC.PL; wood chips from broadleaf forestry sites - 10.BC.PL; walnut shells - 3.BC.PP WS; BC stands for biochar; PL stands for pyrolysis labscale; GL stands for gasification labscale; PP stands for pyrolysis pilotscale; GP stands for gasification pilotscale; 35
Table 25: Sum of PAH and individual PAH results of the biochar gasification samples made river woody debris - 2.BC.GL; spelt husks - 6.BC.GL; wood affected by bark beetles - 7.BC.GL; chestnut wood without tannins - 8.BC.GL; vine prunings - 9.BC.GL; wood affected by bark beetles - 7.BC.GP; and the biochar pyrolysis samples made from coffee husks - 1.BC.PL ; walnut shells - 3.BC.PL; bran 4.BC.PL; Compost screenings - 5.BC.PL; wood chips from broadleaf forestry sites - 10.BC.PL; walnut shells - 3.BC.PP WS; BC stands for biochar; PL stands for pyrolysis labscale; GL stands for gasification labscale; PP stands for pyrolysis pilotscale; GP stands for gasification pilotscale 37
Table 26: PCB results of the biochar gasification pilotscale sample made of wood affected by bark beetles - 7.BC.GP and the biochar pilotscale pyrolysis samples made from walnut shells - 3.BC.PP WS; BC stands for biochar; PP stands for pyrolysis pilotscale; GP stands for gasification pilotscale; 38
Table 27: Dioxins and furans results of the biochar gasification pilotscale sample made of wood affected by bark beetles - 7.BC.GP and the biochar pilotscale pyrolysis samples made from walnut shells - 3.BC.PP WS; BC stands for biochar; PP stands for pyrolysis pilotscale; GP stands for gasification pilotscale; 39
Table 28: pH Values for the Alps4GreenC samples 46

7 References

Bai *et al.,* 2022

Bai S.H., Omidvar N., Gallart M., Kämper W., Tahmasbian I., Farrar M.B., Singh K., Zhou G., Muqadass B., Xu C.Y., Koech R., Li Y., Nguyen T.T.N., van Zwieten L. (2022). Combined effects of biochar and fertilizer applications on yield: A review and meta-analyses, Science of The Total Environment. 808: 152073. https://doi.org/10.1016/j.scitotenv.2021.152073.

Buss *et al.*, 2016

Buss W., Graham M.C., MacKinnon G., Mašek O. (2016). Strategies for producing biochars with minimum PAH contamination. Journal of Analytical and Applied Pyrolysis. 119: 24-30. https://doi.org/10.1016/j.jaap.2016.04.001.

Couto et al., 2013

Couto N., Rouboa A., Silva V., Monteiro E., & Bouziane K. (2013). Influence of the biomass gasification processes on the final composition of syngas. Energy Procedia, 36:596-606. https://doi.org/10.1016/j.egypro.2013.07.068

EBC, 2022

EBC (2012-2023) 'European Biochar Certificate - Guidelines for a Sustainable Production of Biochar.' Carbon Standards International (CSI). Frick. Switzerland. (http://european-biochar.org). Version 10.3 from 5th Apr 2022 (assessed: 15. November 2023)

Ghani *et al.,* 2013

Ghani W. A. W. A. K., Mohd A., da Silva G., Bachmann R. T., Taufiq-Yap Y. H., Rashid U., Al-Muhtaseb A. H. (2013). Biochar production from waste rubber-wood-sawdust and its potential use in C sequestration: Chemical and physical characterization. Industrial Crops and Products. 44: 18–24. https://doi.org/10.1016/J.INDCROP.2012.10.017

Ippolito *et al.,* 2020

*Ippolito J.A., Cui L., Kammann C. (2020). Feedstock choice, pyrolysis temperature and type influence biochar characteristics: a comprehensive meta-data analyses review. Biochar **2**, 421–438. https://doi.org/10.1007/s42773-020-00067-x*

Khan *et al.,* 2019

Khan F., Mahmood S., Ahmad Z., Mahmood T., Nizami Z.A. (2019). Graphene oxide synthesis by facile method and its characterization. Open Journal of Chemistry. 2: 11–15. https://doi.org/10.30538/psrp-ojc2019.0008.

Lee *et al.,* 2016

Lee J.W., Hawkins, B., Kidder, M.K. (2016) Characterization of biochars produced from peanut hulls and pine wood with different pyrolysis conditions. Bioresour. Bioprocess. 3: 15. https://doi.org/10.1186/s40643-016-0092-x

Lower *et al.,* 2023
Lower L., Dey S.C., Vook T., Nimlos M., Park S., Sagues W.J. (2023). Catalytic Graphitization of Biocarbon for Lithium-Ion Anodes: A Minireview. ChemSusChem 16: 202300729. https://doi.org/10.1002/cssc.202300729.

Maschio *et al.,* 1994
Maschio G., Lucchesi A., Stoppato G. (1994). Production of syngas from biomass. Bioresource Technology. 48: 119-126. https://doi.org/10.1016/0960-8524(94)90198-8

Munera-Echeverri *et al.,* 2018
Munera-Echeverri J.L., Martinsen V., Strand L.T., Zivanovic V., Cornelissen G., Mulder J. (2018). Cation exchange capacity of biochar: An urgent method modification. Science of The Total Environment. 642: 190-197. https://doi.org/10.1016/j.scitotenv.2018.06.017.

Oasmaa *et al.,* 2009
Oasmaa A., Solantausta Y., Arpiainen V., Kuoppala E., Sipilä K. (2009). Fast Pyrolysis Bio-Oils from Wood and Agricultural Residues. Energy Fuels. 24: 1380 -1388. https://doi.org/10.1021/ef901107f

Oasmaa *et al.,* 2012
Oasmaa A., Kuoppala E., Solantausta Y. (2012). Fast Pyrolysis of Forestry Residue. 2. Physicochemical Composition of Product Liquid. Energy Fuels. 26: 1275–1283 https://doi.org/10.1021/ef020206g

Pusceddu *et al.*, 2017
Pusceddu E., Montanaro A., Fioravanti G., Santilli S.F., Foscolo P.U., Criscuoli I., Raschi A., Miglietta F. (2017). Comparison between ancient and fresh biochar samples. a study on the recalcitrance of carbonaceous structures during soil incubation. International Journal of New Technology and Research 3: 39–46. https://www.researchgate.net/publication/315691059.

Mukhopadhyay *et al.*, 2022
Mukhopadhyay S., Masto R.E., Sarkar P., Bari S. (2022). Biochar washing to improve the fuel quality of agro-industrial waste biomass. Journal of the Energy Institute. 102: 60-69. https://doi.org/10.1016/j.joei.2022.02.011.

Quicker and Weber, 2016
Quicker P., Weber K., eds. (2023)) Biokohle. Springer Fachmedien Wiesbaden

Sieb-OPTI, 2020
Gallery S., Hüttner A., Turk T., Warning L., Richter F. (2021) Optimierte Verwertung von Siebresten aus Biogutvergärungs- und-kompostierungsanlagen (Sieb-OPTI): Schlussbericht : Projektlaufzeit: 01.07.2018 bis 31.12.2020. Witzenhausen 10.2314/KXP:1810913527

Singh *et al.,* 2010
Singh B., Singh B. P., Cowie A. L. (2010). Characterisation and evaluation of biochars for their application as a soil amendment. Australian Journal of Soil Research. 48: 516. doi:10.1071/sr10058

Singh *et al.,* 2017
Singh B., Dolk M.M., Qinhua S., Camps A.M. (2017). Chapter 3. Biochar pH. electrical conductivity and liming potential.

Safarian et al., 2023
Safarian S. (2023). To what extent could biochar replace coal and coke in steel industries?. Fuel. 339: 127401. https://doi.org/10.1016/j.fuel.2023.127401

Steiner *et al.*, 2016
Steiner C., Guo M., He Z., Uchimiya. S. M. (2016). Considerations in Biochar Characterization. SSSA Special Publication. doi:10.2136/sssaspecpub63.2014.00

Tomcyzk *et al.*, 2020
Tomczyk A., Sokołowska Z., Boguta P. (2020). Biochar physicochemical properties: pyrolysis temperature and feedstock kind effects. Reviews in Environmental Science and Biotechnology. 19: 191–215. https://doi.org/10.1007/s11157-020-09523-3.

Wang et al., 2014
Wang T., Camps-Arbestain M., Hedley M., Singh B. P., Calvelo-Pereira R., & Wang C. (2014). Determination of carbonate-C in biochars. Soil Research. 52: 495. doi:10.1071/sr13177.